HHS Public Access

Author manuscript

Wiley Interdiscip Rev Nanomed Nanobiotechnol. Author manuscript; available in PMC 2017 June 27.

Published in final edited form as:

Wiley Interdiscip Rev Nanomed Nanobiotechnol. 2011 ; 3(6): 620–646. doi:10.1002/wnan.158.

Emerging applications of nanotechnology for the diagnosis and management of vulnerable atherosclerotic plaques

Shann S. Yu[1], **Ryan A. Ortega**[1], **Brendan W. Reagan**[2], **John A. McPherson**[3], **Hak-Joon Sung**[1], and **Todd D. Giorgio**[1,4,*]

[1]Department of Biomedical Engineering, Vanderbilt University, Nashville, TN, USA

[2]Division of Cardiovascular Medicine, Vanderbilt Heart & Vascular Institute, Nashville, TN, USA

[3]Cardiovascular Intensive Care Unit, Vanderbilt Heart & Vascular Institute, Nashville, TN, USA

[4]Department of Chemical and Biomolecular Engineering, Vanderbilt University, Nashville, TN, USA

Abstract

An estimated 16 million people in the United States have coronary artery disease (CAD), and approximately 325,000 people die annually from cardiac arrest. About two-thirds of unexpected cardiac deaths occur without prior recognition of cardiac disease. A vast majority of these deaths are attributable to the rupture of 'Vulnerable atherosclerotic plaques'. Clinically, plaque vulnerability is typically assessed through imaging techniques, and ruptured plaques leading to acute myocardial infarction are treated through angioplasty or stenting. Despite significant advances, it is clear that current imaging methods are insufficiently capable for elucidating plaque composition—which is a key determinant of vulnerability. Further, the exciting improvement in the treatment of CAD afforded by stenting procedures has been buffered by significant undesirable host-implant effects, including restenosis and late thrombosis. Nanotechnology has led to some potential solutions to these problems by yielding constructs that interface with plaque cellular components at an unprecedented size scale. By leveraging the innate ability of macrophages to phagocytose nanoparticles, contrast agents can now be targeted to plaque inflammatory activity. Improvements in nano-patterning procedures have now led to increased ability to regenerate tissue isotropy directly on stents, enabling gradual regeneration of normal, physiologic vascular structures. Advancements in immunoassay technologies promise lower costs for biomarker measurements, and in the near future, may enable the addition of routine blood testing to the clinician's toolbox—decreasing the costs of atherosclerosis-related medical care. These are merely three examples among many stories of how nanotechnology continues to promise advances in the diagnosis and treatment of vulnerable atherosclerotic plaques.

INTRODUCTION

Cardiovascular disease continues to be the leading cause of death in the United States, accounting for 1 of every 2.9 deaths.[1] The development of atherosclerotic plaques is

*Correspondence to: todd.d.giorgio@vanderbilt.edu.

responsible for many of these events, and is characterized by a cascade of events including the accumulation of lipids in arterial walls, oxidation of the lipids, and recruitment of inflammatory cells into these lipid-rich regions.[2] Under the influence of chronic lipid deposition and oxidation, inflammatory activity, and resulting abnormal blood flow and mechanical loading conditions in the region, these plaques may suddenly rupture and lead to a potentially lethal acute event such as a stroke or a myocardial infarction. Therefore, identifying and locating plaques at particular risk of rupture (vulnerable plaques) may potentially provide the basis for therapeutic interventions in the prevention of sudden cardiac death and myocardial infarction.

Despite advances in diagnostic tools, many patients at increased risk for acute coronary events (vulnerable patients) are not identified, as they do not present with any symptoms prior to an acute coronary event.[3] At present, there is no consensus regarding the appropriate treatment of a coronary plaque believed to be at high risk for rupture. Stent implantation, currently used to treat symptomatic obstructive CAD and ruptured plaques in acute myocardial infarctions, may represent a potential therapeutic option for treatment of vulnerable plaques in the future. However, subjecting an asymptomatic patient to the procedural and long-term risks of stenting, including a renarrowing or sudden thrombosis within the stent, is not justified by scientific evidence at this time.[4,5] It is clear that novel cellular and molecular imaging tools are required in order to better assess a patient's risk of potentially life-threatening acute plaque rupture. At the same time, for the mechanical treatment of asymptomatic vulnerable plaques to become a feasible approach, improvements in treatment technologies are required in order to reduce the likelihood of undesirable host responses to implanted materials and unanticipated adverse events, as well as the restoration of physiological vascular function.

CHARACTERISTICS OF VULNERABLE ATHEROSCLEROTIC PLAQUES: MORPHOLOGICAL, MECHANICAL, AND MATERIAL PROPERTIES

From an engineering standpoint, an accurate morphological, mechanical, and material description of vulnerable atherosclerotic plaques is necessary in order to better design treatment tools for their management. It is important to note that each of these categories is interconnected, as changes in morphology and composition of plaques will undoubtedly affect changes in mechanical and material properties of plaques, and vice versa.[6,7]

While the morphological determinants of plaque vulnerability remain difficult to pinpoint conclusively, autopsy studies have suggested that vulnerable plaques are very likely to exhibit some of the following five features: (1) active inflammatory activity, (2) thin fibrous caps and large lipid cores, (3) endothelial erosion and thrombosis, (4) fissured or ruptured caps, and (5) luminal stenosis (>90%).[3,8]

The multiple roles of inflammatory activity in influencing plaque vulnerability are particularly important to note. Under normal conditions, low-density lipoprotein (LDL) particles in the bloodstream and in the arterial wall may become oxidized, producing oxidized LDL (oxLDL), which is rapidly cleared by macrophages in the liver.[9,10] Early in lesion formation, however, the balance between the entry of LDL into the vascular wall and

its efflux becomes disturbed, leading to increased retention of LDL at focal points in the vascular wall. Combined with normal oxidation processes, elevated local levels of oxLDL produces an environment that is chemoattractive to monocytes and T-cells, among others.[10]

The influx of macrophages into an atherosclerotic lesion leads to some major repercussions. Macrophages within a lesion express various scavenger receptors that facilitate endocytosis of lipids and other interstitial debris. This activity eventually results in transformation of macrophages into foam cells, and their further activation leads to apoptosis—usually triggered by high local concentrations of oxLDL, TNF-α, Fas ligand, intracellular accumulation of free cholesterol, or hypoxia—contributing to the gradual expansion of the necrotic core.[11,12] The production of matrix metalloproteinase (MMP)-8 and -9 by monocytes/macrophages in response to pathological stimuli leads to degradation and destabilization of the local extracellular matrix, increasing the likelihood of plaque rupture.[13–17] For these reasons, atherosclerosis is commonly thought of as an inflammatory disease, and this classification continues to guide burgeoning work in this area.[18]

Mechanically, the formation of a plaque is characterized by intimal thickening, leading to a dramatic increase in intimal stiffness and elastic modulus, relative to normal arteries.[7,19–24] (Figure 1(a)). Conversely, the media and adventitia of the diseased blood vessels become abnormally softer than their corresponding layers in normal arteries. Therefore, changes in the layer-by-layer modulus of pathological arteries show an opposite pattern to normal arteries where the modulus gradually increases from intima to adventitia. This change in the layer-by-layer modulus of arterial wall can be explained by a theory with respect to progressive arterial remodeling from intimal thickening to outward expansion[20] in response to pathological stimuli (Figure 1(b)). In normal arteries, the intima provides an elastic layer of path for blood flow, which is supported by the media, while the adventitia supports the structural integrity of vessel wall. Therefore, the modulus increases gradually from intima to adventitia. Under pathological situations, the formation of lesion with fibrous caps contributes to a dramatic increase in the stiffness of the intima, resulting in a significant increase in the modulus of intima. Then the artery expands outward to increase the lumen for restoration of proper blood flow, which was decreased substantially by intimal thickening. Expansion beyond the limits required for maintenance of tissue integrity often results in rupture of the outer layer.

Pathological observations and experimental studies indicate that MMP expression is increased in high stress sites of such arteries.[25] At the same time, rupture of the vessel wall with plaque destabilization occurs in arteries that have undergone outward remodeling, suggesting that degradation of matrix by MMPs may eventually lead to weakening and destabilization of the media and adventia, as indicated by decreases in modulus of middle and outer layers. In addition, the development of these properties is partially influenced by the luminal shear stresses. In particular, stenotic regions experience increased shear stresses, resulting in changes in endothelial gene expression and integrin-ECM binding affinity.[6] Further, regions of lower shear stress may form downstream of stenotic regions, resulting in upregulation of VCAM-1, C-reactive protein (CRP), and IL-6 by endothelial cells. The expression of VCAM-1 and IL-6 increases the recruitment of inflammatory cells into the local interstitium, and IL-6 can further regulate the production of MMPs.[26]

From a materials standpoint, local porosity and compliance are the most important parameters. Plaque endothelium is not fenestrated, but is generally known to exhibit higher permeability to nanoparticles than healthy endothelium.[27] Further, endothelial cells are also known to be capable of transcytosis, providing an alternative route for translocating circulating nanoparticles to the interstitium.[28] Local compliance is governed primarily by the variations in mechanical properties across the different tissue layers in the vasculature, including the pathologic structures such as the necrotic core, as well as the percentage composition of each of these structures. Mechanical properties can be heterogeneous even within the same plaque, leading to unpredictable stretch-relaxation behaviors under dynamic, pulsatile blood flow conditions.[29] It is well understood that when two adjacent tissue components exhibit a significant level of compliance mismatch, such blood flow conditions can rapidly develop fractures in the interface between these components can escalate into deadly aneurysms.[30]

Taken altogether, vulnerable plaques can be identified by abnormal local inflammatory and proteolytic activity, thrombosis, heterogeneity of mechanical properties in the local vascular wall, and an increase in interstitial perfusion.

A CLINICAL PERSPECTIVE: DIAGNOSIS AND IMAGING OF VULNERABLE PLAQUES TODAY

With the recognition that clinically silent, nonobstructive (<70% luminal stenosis) CAD may present a great risk of acute myocardial infarction and sudden cardiac death,[31–34] cardiologists are increasingly interested in identifying vulnerable plaques. However, in clinical practice, both noninvasive testing and invasive imaging are designed to identify obstructive coronary artery disease, which can provide important prognostic information and also guide decisions regarding coronary revascularization. The use of currently available imaging modalities used in clinical practice to identify coronary plaques with morphologic features consistent with a vulnerable plaque phenotype is thus somewhat limited. However, as interest in the identification and treatment of vulnerable plaques increases, there have been significant recent advances in intra-coronary imaging of inflammatory plaques, which are summarized below.

The imaging modalities are divided into non-invasive and invasive techniques. While noninvasive techniques are more applicable to the asymptomatic patient with nonobstructive coronary disease, they are generally limited by cardiac movement and the tortuous nature of coronary arteries. Because of direct visualization of the coronary arteries, invasive techniques allow improved resolution but involve increased risk to the patient and are not suitable for screening of asymptomatic patients.

Noninvasive Imaging

Cardiac applications of computed tomography (CT) have progressed rapidly with technologic advances. Electron-beam CT was first used to predict the likelihood of coronary events by identifying coronary calcification which correlates with calcific plaque burden. With the development of fast multidetector CT (MDCT), the coronary artery lumen as well

as the vessel wall can be assessed. MDCT has the capacity to examine plaque composition by using density measurements but is limited by blooming artifact and overlap of CT attenuation values between lipid-rich and fibrous noncalcified plaque.[35] The recent introduction of dual source CT has improved temporal resolution and accurately identified lipid plaques compared to intravascular ultrasound (IVUS) without excluding calcified plaques.[36] On the basis of these capabilities, CT can accurately determine overall plaque burden and characterize arterial remodeling. CT still has significant limitations related to radiation exposure, resolution, and soft tissue contrast; but it holds great promise as techniques continue to improve.

Magnetic resonance imaging (MRI) provides excellent soft tissue contrast and does not expose the patient to ionizing radiation. MRI has been extensively studied in the imaging of inflammatory plaques in the carotid arteries and has shown strong correlations with histology in the identification of the lipid core and fibrous cap.[37] Unfortunately, low spatial resolution has hindered its applicability to coronary artery imaging. Gadolinium-based contrast agents have been used to extend MRI capabilities to include smaller blood vessels, but because of concerns with renal toxicity, alternative materials such as superparamagnetic iron oxides have received much interest.[28,38–42] Additionally, nanoparticulate contrast agents are advantageous because they are avidly recognized and uptaken by macrophages regardless of surface chemistry, and vulnerable plaques tend to exhibit high macrophage contents.[28,43–51] Finally, another disadvantage of MRI is that many patients are not compatible with this procedure because of metallic medical implants including pacemakers and implantable cardiac defibrillators.

Positron emission tomography (PET) and single photon emission computed tomography (SPECT) require radioactive tracers, allow less spatial resolution than MRI, and expose the patient to ionizing radiation, but are more sensitive than MRI for detection of plaque biomarkers.[52] Because the disadvantages of MRI fall into the advantages of PET/SPECT, and vice versa, multimodal contrast agents that can be detected through multiple imaging platforms are of much interest. For example, Nahrendorf et al. synthesized an iron oxide nanoparticle labeled with ^{64}Cu PET tracer to enable bimodal imaging of the contrast agent via PET/MRI.[48] Following *in vivo* imaging studies, plaque material was digested and analyzed by flow cytometry, and indicated that the nanoparticles were predominantly uptaken by macrophages.

Imaging with transcutaneous ultrasound has several advantages, including its safety, cost, and wide availability. With the use of contrast agents, ultrasound can detect the presence of intraplaque neovascularization. As inflammatory plaques enlarge, they require their own blood supply and develop a mature network of arterioles (vasa vasorum) on the adventitial surface of the vessel.[53] Contrast-enhanced ultrasound has the ability to detect the presence of vasa vasorum.[54] Currently, this application is limited to superficial vessels such as carotid arteries.

Molecular imaging using radionuclides has potential for adding functional information about inflammatory coronary plaques to anatomical information obtained from other imaging

modalities. While promising, thus far the data is still limited[55–57] and not ready for clinical application.

Invasive Imaging Techniques

Coronary angiography is the most common invasive technique used, but only assesses the vascular lumen, causing deficiencies in identifying mild plaques, evaluating vessel size, and assessing plaque characteristics.

Intravascular ultrasound (IVUS) has traditionally been utilized to assess the anatomical characteristics of plaque and disease burden often underestimated by angiography because of positive remodeling. Although the resolution of IVUS (100–250 μm) does not allow for identification of the thin fibrous cap (estimated 23 ± 19 μm by histology of ruptured plaques),[58] the presence of the necrotic core as identified by large echolucent areas or attenuation of the echo signal in noncalcified areas may have clinical relevance.[59–61] However, gray-scale IVUS is limited in its ability to characterize plaque morphology. The addition of integrated backscatter analysis to grayscale IVUS, called radiofrequency-IVUS (RF-IVUS) can provide improved characterization of the individual components of atherosclerotic plaque including fibrotic tissue, fibrofatty tissue, necrotic core, and dense calcium.[62–65] A prospective study of patients with high-risk coronary artery disease recently demonstrated that RF-IVUS can identify coronary plaques with a morphologic phenotype (TCFA) that are at increased risk for subsequent cardiovascular events.[66]

Optical coherence tomography (OCT) measures back-reflected infrared light and provides the highest resolution (5–20 μm) of all the invasive imaging techniques.[67,68] Because of its excellent resolution, histopathological correlations have demonstrated sensitivities of 87–92% and specificities of 94–100% in identification of various plaques.[67] Although imaging acquisition procedures are improving, its clinical application is currently limited because of signal attenuation by blood necessitating prolonged, proximal occlusions to screen long arterial segments. Intracoronary optical frequency domain imaging (OFDI), a next-generation OCT-derived imaging method, overcomes some of these limitations, with a substantially increased speed of image acquisition when compared with first-generation time-domain OCT.[69] However, both OCT and OFDI have a somewhat limited penetration and are thus unable to adequately image beyond the inner fibrous cap and lipid core in larger arteries.

Intravascular MRI depicts components of atherothrombotic plaque including lipid, fibrous tissue, calcium, and thrombus formation.[70,71] There is potential for combination with cellular and molecular targeting.[72] *In vivo* MRI catheters have had limited human testing,[73] and real time endovascular MRI imaging continues to advance experimentally,[74] but intravascular MRI is not a clinical reality yet.

Optical imaging is commonly used in the lab to verify the reliability of plaque biomarkers because of its widespread availability, ease of use, and the lack of ionizing radiation exposure to the user. However, the application of this technique to *in vivo* imaging in humans is difficult because of tissue autofluorescence and optical attenuation and scattering —effects that are less marked in the near-infrared window of 650–900 nm.[75,76] Therefore,

the success of optical imaging approaches for human applications will require the design of probes that exhibit absorbance or excitation and emission spectra that occur within this 300 nm window. Indeed, near-infrared spectroscopy (NIRS) analyzes the chemical composition of plaque components based on the amount of absorption at different wavelengths. Further, near-infrared spectroscopy (NIRS) catheters enable assessment of intravascular chemical composition, and have been successfully employed to identify lipid-core plaques in human patients.[77,78] The ability of NIRS to identify the chemical composition of plaque components has also been validated with histologic correlations[79–81] and is currently being evaluated in multiple trials including as a combined imaging technique with IVUS. Because NIRS is unable to elucidate tissue structures, the combination of NIRS with IVUS enables correlation of plaque composition with tissue structure on one platform, and has been recently demonstrated in humans.[82]

Angioscopy and thermography also deserve mention but have failed to show clinical utility in the identification of vulnerable plaques despite initial promising results.

IMAGING VULNERABLE PLAQUES WITH NANOTECHNOLOGY

One of the main challenges in the prevention of myocardial infarctions and strokes involves the identification of plaques at highest risk of rupture that are in most need of prophylactic therapeutic intervention. As discussed earlier, plaque composition appears to be the primary determinant of plaque instability.[3,8] As a result, the primary molecular imaging targets for the identification of vulnerable plaques includes markers of inflammation, thrombosis, apoptosis, or angiogenesis.[83,84] Advances in noninvasive imaging approaches are revolutionizing the ability to spatially pinpoint the locations of these vulnerable plaques in the clinic. Nanotechnology has led to the creation of several nanoparticle platforms that can be applied as contrast agents for a range of noninvasive imaging modalities.

Recently, a library of nanoparticle platforms has been developed for molecular imaging of plaque biomarkers (Table 1). This table is not meant to be an exhaustive list, but rather, highlights key developments in this area that have been used to image vulnerable plaques *in vivo* or *ex vivo.* Below, we highlight novel approaches for imaging cell receptors and cell types, as well as protease activity in vulnerable plaques. A word of caution must be added when interpreting the vast collection of data in this area, as an ideal animal model that exhibits intrinsic plaque destabilization and rupture remains undeveloped. The apoE$^{-/-}$ mouse—likely the most widely used small animal model of atherosclerosis—is known to develop atherosclerotic lesions spontaneously, but generally require extrinsic triggers or exogenously administered means in order to trigger plaque rupture.[85] The lack of a robust animal model that develops atherosclerotic lesions closely mimicking plaque destabilization and rupture in human patients remains one of the largest barriers in the translation of these promising results from the bench to the bedside.

Imaging Cell Receptors in Atherosclerosis

As described above, atherosclerosis is generally classified as an inflammatory disease, and as a result, a range of inflammatory biomarkers have been implicated in plaque destabilization. These biomarkers include the adhesion molecules ICAM-1, VCAM-1, and

E-selectin, as well as macrophage markers such as CD40, CD68, dextran receptors, Mac-3, and scavenger receptors MSR-A/MSR-B.[12,48,113–117] These biomarkers have been targeted in a variety of studies involving nanoparticle-mediated molecular imaging (Table 1).

Work in the Fayad and Tsimikas groups has produced a library of synthetic micelles and lipoprotein mimics for imaging of some of these biomarkers, including oxidation-specific epitopes[47,92–94,103,104,107,118] (Figure 2). Imaging oxLDL is of particular interest because it allows for the identification of oxidized epitopes in the vascular wall, and when used in tandem with measurements of circulating oxLDL—a well-developed paradigm for assessing the risk of coronary events—demonstrates a biomarker and an imaging application based on the same epitope.[103,104,119] For imaging applications, contrast agents are incorporated into the nanoparticles in two ways. In the first method, phospholipids are covalently modified with gadolinium chelates or fluorescent tags, and then used in preparation of antibody-displaying micelles.[92,103] As a result, contrast agents are displayed on the nanoparticle surface. In a second method, contrast agents are incorporated into the core of the micelles. This is possible because a variety of contrast agent nanocrystals, including quantum dots, iron oxides, and gold nanoparticles are synthesized in large quantities and at high monodispersity in organic solvents, but remain capped by hydrophobic surfactants.[120–122] Therefore, inclusion of such nanocrystals in micellization processes encapsulates them with phospholipids.[93,95] After micellization, membrane proteins such as ApoA-I can be incorporated into the phospholipid monolayer in a single buffer change step, producing mimics of high-density lipoprotein.[95]

Multimodal contrast agents can be constructed through the marriage of the two approaches described above.[95] Alternatively, dextranated iron oxide nanoparticles can be surface-modified with contrast agents such as the PET tracer ^{64}Cu, in order to enable PET/MRI imaging of plaque biomarkers.[48] Both of these platforms have been further functionalized with antibodies and peptide mimics for molecular imaging.[103,108,109,123]

The Johnston group recently demonstrated a ‘nanorose’ platform for NIR fluorescence and photothermal optical coherence tomography (OCT) imaging of macrophages in a rabbit model of atherosclerosis.[87,124] To synthesize the contrast agent, 2 nm monolayers of Au were grown on iron oxide nanoparticles with dextrose as a reducing agent, yielding dextran-coated iron oxide/gold nanoclusters. The close proximity of the singlets in the cluster enhances NIR absorbance of the system.[87] Further, because of the thinness of the Au layers, iron oxide particles are placed in close proximity to one another, leading to higher R_2 relaxivities with clustered particles versus with dispersed particles.[125] The dextran coating facilitates uptake of the nanoroses by macrophages, enabling inflammatory cell-laden plaques to be easily imaged.[117]

Imaging Protease Activity in Atherosclerosis

Increased activity of extracellular proteases such as MMP-2, -8, and -9; and cathepsins B, K, L, and S has been implicated in plaque destabilization and rupture.[16,17,21,126–130] As a result, probes for imaging proteases activities are expected to improve the detection of vulnerable plaques in the clinic.

The Weissleder group pioneered NIR fluorescence beacons for imaging protease activity in plaques, where polymers are modified with NIR fluorophores in such a way that the dyes exhibit self-quenching in the absence of protease activity.[127,131,132] Following protease degradation of linkers holding the fluorophores in proximity to one another, release of the fluorophores results in the disappearance of the self-quenching effect and an increase in NIR emission, which has been used to specifically image active cathepsin B, D, and K and MMP-2 and -9.[127,131,133,134]

However, it is worthwhile to note that a drawback behind these approaches involves the use of organic fluorophores, which in general, exhibit much lower quantum yields and higher photobleaching effects versus fluorescent nanoparticles such as quantum dots. While these novel ‘smart’ probes have led to promising results from mouse models (Table 1), their successful application in the clinic will necessitate highly sensitive fluorescence detectors and brighter excitation sources, counteracting the significantly higher optical attenuation and scattering effects expected.[135]

As an alternative to using environmentally activatable organic dyes, Chang et al. presented a protease-activatable fluorescence probe based on quantum dot-Au nanoparticle complexes.[136] In this scheme, Au colloid was attached to CdSe/CdS QDs via MMP-1-degradable peptide linkers. At close proximity (<10nm), the gold colloid absorbs quantum dot emission via a FRET mechanism. However, the presence of MMP-1 results in release of the quenching Au colloid from the QD surface, and ‘activation’ of QD emission. Recent work by the same group has led to NIR-emitting quantum dots that are likely more suitable for clinical applications because of their optical properties.[137] Other approaches have also been followed in order to obtain NIR-emitting QDs, but because of the presence of cadmium in most of these structures, cytotoxicity remains a primary concern and roadblock to potential applications of this technology in humans.[135,138–143]

While a majority of approaches to actively image plaque biomarkers utilize one targeting ligand (peptide, protein, or antibody) to target the biomarker directly, a promising new approach developed in the Giorgio and Bhatia groups can potentially enable specific imaging of plaques that exhibit two separate characteristics.[101,144,145] Originally designed for tumor imaging, this approach is termed ‘proximity-activated targeting’ (PAT), where nanoparticle surfaces are functionalized with two distinct molecular ligands necessary for pathologically specific targeting. Specifically, quantum dots were surface functionalized to include a polyethylene glycol (PEG) chain interrupted by the peptide target of matrix metalloprotease-7 (MMP-7) and a second, shorter structure that terminated in folic acid. The construct was targeted to breast cancer metastases through the folate ligand that was initially concealed by the peptide-bridged PEG (Figure 3(a)), which remained biologically inactive until exposure to MMP-7 (Figure 3(b) and (c)). MMP-7 degradation of the peptide bridge uncoupled the passivating PEG structure from the construct, revealing the folate ligand only in the proximity of the tumor[144,146] (Figure 3(d)). The modular approach used in the construction of these contrast agents enables other nanoparticles to be used in the core, such as iron oxide, for MRI.[101] Other proteases and receptors can also be targeted using this approach simply by changing the cleavable peptide unit and the peptide targeting unit used in the final construct.

Advantages of Nanoparticulate Contrast Agents in Vulnerable Plaque Imaging

Nanoparticles provide an array of advantages in plaque imaging versus their small molecular probe counterparts, including circulation half-life, site selectivity, and modular design.

Because most nanoparticulate contrast agents for plaque imaging applications exhibit diameters above 10 nm, they are generally too large to be filtered through the glomeruli in the kidneys, where pores exhibit cutoff diameters of 8 nm or less.[147] Small molecule contrast agents are easily filtered through the kidneys, and are rarely reabsorbed, leading to much smaller circulation half-lives than nanoparticles. Circulating nanoparticles tend to be cleared through the reticuloendothelial system (RES), also known as the mononuclear phagocyte system (MPS), which includes phagocytic cells residing in the spleen and the liver, among other organs.[148,149] The kinetics of nanoparticle clearance through this route can be significantly slowed through the appropriate use of polymeric surface coatings such as poly(ethylene glycol) (PEG) or poly(hydroxypropyl methacrylate) (HPMA), which reduce opsonization of nanoparticles.[150,151]

Site selectivity can be mediated to some extent by the enhanced permeation and retention (EPR) effect in a similar fashion as seen in cancer, as vulnerable plaques tend to exhibit multiple fissures in the fibrous cap, as well as impaired endothelial function.[3,152,153] Although the EPR effect has been conclusively demonstrated in induced tumors in animal models, to our knowledge, only one observation of this effect has been reported in humans to date.[154] Further, the larger size of nanoparticles versus small molecular probes provides a platform for multivalent coupling of ligands for active cell targeting, such as antibodies and peptides, which improves affinity of the nanoparticles for their molecular targets.[155]

Finally, nanoparticulate contrast agents are known for their modular design, in that the contrast agents, targeting agents, stabilizing polymers, and other functionalities can be easily tuned during synthesis. Several schemes have already been described earlier in this review. The simplicity in generating functional nanoparticulate contrast agents has also led to the facile synthesis of multimodal contrast agents.[48,86,87,95,124]

Ongoing advances in nanoparticle synthesis and processing processes have led to materials with novel properties appropriate for applications in this area, including iron oxide nanoparticles with R_1 relaxation and biocompatible silicon-based quantum dots.[156,157] ‘Smart’ environmentally sensitive dendrimer-based nanobeacons have been synthesized by the Matrisian group, which emit NIR fluorescence only in the presence of proteases of interest.[158,159] This platform can also be loaded with small molecule drugs, producing a ‘theranostic’ platform capable of site-specific therapy and imaging. For all of these reasons, nanotechnology will continue to be a significant player in the imaging of vulnerable plaques.

THE *IN VITRO* DIAGNOSTICS REVOLUTION: APPLICATIONS OF NANOTECHNOLOGY IN BLOOD TESTING AND BIOMARKER DETECTION

Rapid, accurate, noninvasive measurement of circulating, plasma-based biomarkers potentially provides powerful information for diagnosis and risk stratification of patients with cardiovascular diseases. A few such biomarkers that are already being measured in the

clinic for this purpose include C-reactive protein (CRP), lipoprotein (a), myeloperoxidase, oxLDL, troponin I, and MMP-9, among others, as reviewed elsewhere.[160,161] However, it is clear that no single biomarker can lead to conclusive risk assessment. Rather, assessment of a small library of biomarkers is necessary to accurately diagnose a patient's susceptibility to potentially lethal acute cardiac events.[161]

A challenge is that current methods to measure concentrations of circulating biomarkers in the clinic generally require expensive and impractical equipment, long sample handling and preparation times, significant reagent usage, and moreover, can only assay one analyte at a time. Nanotechnology has led to the development of several platforms that hold promise in tackling all of these challenges.

For example, nanomaterials functionalized with antibodies specific for a biomarker of interest have been used in novel experimental immunoassays.[162–168] These novel immunoassays are sensitive enough to detect analytes at femtomolar concentrations, primarily because of the significantly higher biosensing surface area offered by immobilization of the sensing elements—the antibodies—to nanostructured surfaces. Further, most of such nanoparticle-based biosensing platforms also possess physical properties that change based on the aggregation state of the nanoparticles. Specifically in the presence of analytes of interest, the nanoparticles aggregate, producing significant changes in optical, magnetic, or fluorescent properties of the system. In some cases, detection is possible even in unfractionated blood, thereby greatly reducing sample processing time.[166,169,170]

Microfluidics technology has also miniaturized immunoassays, in terms of sample and reagent volumes as well as equipment, enabling multiplexed antigen detection in sub-microliter volumes at unprecedentedly low costs.[171–173] Smaller, microfluidics-sized versions of the highly technical equipment usually required for nanoparticle-based immunoassays in the laboratory have also been recently been constructed, including flow cytometers,[174,175] spectrophotometers,[176] magnetic relaxometers,[177,178] and dynamic light scattering (DLS) analyzers,[179,180] among others. Integrating nanotechnology-enabled immunoassay schemes with microfluidics holds promise in revolutionizing clinical detection of libraries of circulating biomarkers that collectively report the existence of vulnerable plaques.

Soman et al. described a method for flow cytometric detection of blood-borne analytes based on agglomeration of antibody-functionalized quantum dots.[163,181] As nanoparticle agglomerates scatter light more effectively than individual, dispersed nanoparticles,[182] the light scattering instrumentation equipped on standard flow cytometers are capable of detecting the presence of analytes based on the appearance of high-scattering species following as little as 60 min incubation time. By producing a library of quantum dots—each population displaying antibodies for a different target—and identifiable by a different emission wavelength range, analytes can be 'bar-coded', enabling multiplexed detection of a library of analytes through fluorescent emission versus light scattering plots.[181] The authors detected vascular endothelial growth factor A and angiopoietin-2 in saline, down to a

femtomolar sensitivity limit.[181] However, detection capabilities in whole, unfractionated blood were not investigated.

Hirsch et al. demonstrated detection of analytes in whole blood using antibody-functionalized silica-gold core-shell nanoshells.[162,166] These nano-shells absorb at wavelengths in the near-infrared (NIR) window of 700–1000 nm—where optical attenuation and scattering effects because of blood components are minimized[79] (Figure 4). After rabbit IgG was mixed into whole human blood, nanoshells agglomerated, resulting in a red-shift in plasmon resonance of the system within 15–30 min. This effect is also accompanied by a decrease in peak extinction of the system.[166] A light, portable, single-wavelength LED-based 'spectrophotometer' was constructed to enable translation of the nanoshell immunoassay to low-resource, point-of-care applications.[183]

Ibraimi et al. developed a ~5 min immunoassay that works in a similar fashion as these methods, involving the use of polyclonal anti-CRP-functionalized silica microparticles and monoclonal anti-CRP-functionalized superparamagnetic iron oxide nanoparticles.[170] The silica microparticles generally sediment within 5 min even in the absence of agglomeration with CRP. However, when CRP is present, iron oxide nanoparticles become incorporated into the precipitate, increasing its magnetic permeability. A portable magnetic permeability detector was used to quantify concentration of CRP in as little as 4 μL of whole blood, and the sensitivity and accuracy of the method was comparable to several commercially available reference methods.[170]

Magnetic nanoparticle-based immunoassays can also be carried out with optical detectors, as the general principle of analyte-mediated nanoparticle agglomeration results in increased light scattering properties and extinction in the system.[182] In such setups, the nanoparticle surface simply provides a vehicle for analyte immobilization, while the magnetic properties enable facile handling and isolation of the particle-analyte complexes.

Recently, this scheme was combined with a total internal reflection (TIR) detector to enable quantitative detection of troponin I in human serum and plasma down to sub-picomolar concentrations.[184] In this work, Bruls et al. preloaded a microfluidic chip with anti-troponin I-functionalized magnetic nanoparticles, and used a magnetic field to capture the nanoparticles during sample loading. Magnetic actuation of the nanoparticles in the presence of the sample enables quick mixing and formation of nanoparticle-analyte complexes within 4 min. The TIR sensor surface is also pre-functionalized with anti-troponin antibodies, enabling high-affinity interactions between the complexes and the surfaces. Application of a magnetic field removes excess nanoparticles prior to optical detection of analyte.[184]

The McDevitt group developed microfabricated chips consisting of arrays of singly confined microparticles, each functionalized with a different antibody for an analyte of interest.[172,185,186] The design of the immunoassay is not very different from that of a sandwich ELISA, except in this case, porous agarose microparticles serve as a scaffold for attachment of capture antibodies. After flowing sample through the beads, application of fluorophore-conjugated detection antibodies and rinsing resulted in quantitative readout of analyte concentrations.[172] This approach has been used to screen human patients for

biomarkers of acute myocardial infarction through measurements of CRP, myoglobin, and myeloperoxidase in salivary samples.[185]

Buch and Rishpon coated screen-printed carbon electrodes with a film of multiwalled carbon nanotubes (MWCNTs), forming a surface for quantification of CRP in human serum by electrochemical immunoassay.[187] Like the immunoassay above, this immunoassay was not very different from a sandwich ELISA in idea. The difference is that quantification of CRP concentration is achieved by monitoring the electrochemical potential at the electrodes, which varies based on the oxidation of the HRP substrate TMB. Therefore, the MWCNT film was further modified with anti-CRP as a capture antibody, while an HRP-conjugate anti-CRP was used as a detection antibody. Application of human serum, followed by wash steps, then the detection antibody and then TMB substrate, quantified CRP down to 0.5 ngmL^{-1}, compared to 10 ng mL^{-1} when the MWCNT film is not present.[187] This difference in detection limit is attributed to the enhanced electrochemical reactivity of peroxides at CNT-modified electrodes, as reviewed elsewhere.[188] The authors reported assay time to be around 10 min.

Given the predominance of costly, time-consuming ELISAs for measuring circulating biomarker levels in the clinic today, the advantages offered by these novel nanotechnology-based immunoassays will make biomarker-based blood diagnostics much more accessible to the public. Further, the rapid assay times offered by these new approaches will enable their routine use, multiple times daily, to track the prognosis of the highest risk patients and enable strategic therapeutic intervention.

A CLINICAL PERSPECTIVE: FUTURE DIRECTIONS FOR THE TREATMENT OF VULNERABLE ATHEROSCLEROTIC PLAQUES

The development of drug eluting stents has revolutionized the treatment of obstructive CAD (Table 2). The initial alternative to open heart surgery for mechanical revascularization was percutaneous transluminal coronary angioplasty with balloon expansion. However, because of problems with acute vessel closure and restenosis,[189–191] the coronary stent was developed with bare metal providing scaffold to prevent closure and recoil.[192] There was rapid adoption of percutaneous coronary interventions (PCI) using bare metal stents (BMS), and target-lesion revascularizations (TLR) were reduced from 25–35% with balloon angioplasty to 10–15% with BMS.[193] Drug eluting stents (DES), developed to prevent the in-stent neointimal hyperplasia leading to restenosis in BMS,[194–196] resulted in a further reduction in TLR to 4–6%.[197–199] However, initial enthusiasm for DES was dampened in 2006 with evidence of a small, but significant, increase in stent thrombosis.[200–202]

The basic components of a DES are the stent platform, a polymer that elutes the drug from the stent surface, and the drug. CYPHER and TAXUS, the first generation drug eluting stents, have stainless steel platforms and elute the antiproliferative agents sirolimus (an immunosuppressant) and paclitaxel (an antineoplastic agent), respectively. The drugs are released by diffusion from nonbiodegradable polymers. Although similar in many respects, sirolimus-eluting stents have superior restenosis rates compared to the paclitaxel-eluting stents because of multiple differences including underlying stent design, polymeric coating,

mechanism of drug action, drug-release kinetics, and drug distribution across the vessel wall.[203]

As concerns of stent thrombosis in first generation DES were raised, one of the major considerations was the impaired endothelization by antiproliferative drugs resulting in blood exposure to a thrombogenic stent strut. Stent thrombosis can also be precipitated by patient-related factors (including diabetes, malignancy, renal failure, poor response to antiplatelet therapy), inadequate duration of antiplatelet therapy, lesion characteristics, and procedural factors (inadequate stent expansion, incomplete stent apposition). Also although greatly reduced, in-stent restenosis (ISR) still occurs in DES albeit with a different mechanism from ISR in BMS.[204]

In order to address some of these concerns, second generation DES (Endeavor, XIENCE) were developed. The cobalt chromium stent platform of the second generation DES allows thinner struts which may enhance endothelial coverage, reduce restenosis and improve deliverability.[205–207] Drugs from the limus family similar to sirolimus are used as the antiproliferative agents. Also because of mounting evidence of the negative role of the polymers used in first generation DES, manufacturers utilized alternative biocompatible polymers which cause less inflammation. Although the new polymers are different from the first-generation DES polymers, second-generation DES in the United States do not employ bioabsorbable polymers. Early comparisons of first and second generation DES have been conflicting, but suggest that second-generation DES are at least as effective, and in the SPIRIT IV trial, the XIENCE stent was demonstrated to be superior to the TAXUS stent.[208]

Given the continued shortcomings of currently available DES, there are multiple other stent innovations currently under investigation. Some technologies have focused on addressing the negative effects of polymers with the development of biodegradable polymeric DES or nonpolymeric DES. Early results comparing these technologies, available commercially in Europe, are most promising for the nonpolymeric DES.[209,210] Because of inherent limitations of DES, biodegradable and bioabsorbable stents are also under development and undergoing preclinical and clinical trials.[211–215] These stents have the potential advantage of degrading or eroding completely over time, allowing for short-term drug delivery to the vascular wall, while avoiding long-term exposure of the stent to pro-inflammatory components in the bloodstream.[215] While preliminary results appear promising, some of the polymeric materials used in these stents, including poly-L-lactic acid and poly-D,L-lactide, may be degraded and eroded into small particles that can be phagocytosed.[214,215] The phagocytosis of these particles have been previously shown to trigger superoxide production by the phagocytes.[216] Despite this possibility, the investigators of the ABSORB stent have not reported any significant inflammatory responses to the implant within 2 years of implantation, and only time will tell if these responses will arise later on in the lifetime of the stent.[215]

Currently, these stent technologies are only applicable to the treatment of obstructive CAD, and they have not been rigorously evaluated for the treatment of nonobstructive vulnerable plaque. As little is known about the lesion-specific risk of future cardiovascular events in high-risk plaques, implantation of a coronary stent in a clinically silent lesion—in order to

prevent a future event—is not justified at this time. The recently completed PROSPECT study (Providing Regional Observations to Study Predictors of Events in the Coronary Tree) demonstrated that the majority of initially asymptomatic, unstented plaques that led to major coronary events within three years featured thin fibrous caps, minimal luminal areas of ≤4mm^2,and ≥70% plaque burden.[66] There are now ongoing pilot studies utilizing stents specially designed for use in nonobstructive coronary plaques which may provide insight into the feasibility of such an approach.[217] Perhaps with continued advancement of stent technology, stents to safely and effectively treat vulnerable plaques will become a reality.

NANO APPROACHES IN THE DESIGN OF NEXT-GENERATION STENTS

Arterial stenting has been one of the most rapidly adopted treatments for coronary and peripheral artery disease.[218] However, unforeseen problems with DES have necessitated further investigation and advancement of stent technology. One of the primary concerns is the significant increase in the occurrence of late stent thrombosis months, even years after implantation of DES as compared to BMS. It is believed that the degradation products of DES, primarily large, poorly biocompatible polymer fragments, are the main contributor to thrombosis and undesired inflammatory events.[219,220] Furthermore, the antiproliferative agents used in DES, when delivered through the current mechanism, can be too effective and prevent the necessary long-term formation of new endothelium.[221]

Drug-Bearing Nanofilms and Nanoparticles

There are many techniques and materials in nanotechnology that may be utilized to address the current problems with DES. The implementation of these nanoscale tools has given rise to the next generation of DES that possesses a larger degree of material complexity and leverage stent coatings with nanoscale modifications designed to enhance biocompatibility. Nanoscale components made from biodegradable polymers for the next generation of DES improve biocompatibility by releasing degradable products that are more biocompatible and less inflammatory than the first-generation DES.[222]

One novel approach utilizes a chitosan film, containing drug loaded poly(D,L-lactic-*co*-glycolic acid) (PLGA) nanoparticles, as a metal stent coating material.[222] These materials have multiple advantageous properties not present in the first generation of DES. First, PLGA nanoparticles can be made easily, rapidly, and in a scalable fashion using oil-in-water emulsification, which can be done in a single stage synthesis.[223] Also, nanoparticles are tunable to control the time period and kinetics of local drug release.[224,225] The presence of two drug loadable vehicles (the nanoparticles and the film itself) provides the opportunity to utilize two drugs that may exhibit different hydrophobicity (which might normally be incompatible in a single device) and tailor the release kinetics of both of these drugs, primarily by altering the degradation rate of chitosan film. The use of a biomolecule-based drug delivery vehicle—a chitosan film—reduces the likelihood of release of large polymer fragments as the film degrades. The nanometer dimensions of the polymeric particles is specifically advantageous for reducing immune responses that can be often triggered by large polymer fragments.[222]

Another next-generation stent design utilizes an inorganic drug eluting coating material comprised of carbon nanoparticles embedded in a thin film of glassy, polymeric carbon.[226] The nanoparticles and carbon matrix create a bioinert, porous coating with favorable elasto-mechanical properties. The porosity of the surface increases the surface area for adsorption of drugs into the construct. The drug release from the carbon matrix can then be specifically tailored by altering the pore size in the coating. This particular study found that paclitaxel loaded carbon—carbon nanoparticle coated stents shows lower mean injury, better endothelialization, and less restenosis than paclitaxel loaded PLGA coated stents, indicating improved biocompatibility for the inorganic coating.[226]

Other stent modification approaches rely on the mechanical and geometric properties of the surface coating to improve re-endothelialization. Using an extracellular matrix-mimicking nanofibrous matrix of nitric oxide-releasing peptide amphiphiles, selective recruitment of endothelial cells was demonstrated, in competition with smooth muscle cells.[227] By utilizing nanofibers 8–10 nm in width and several microns in length, the coating was also capable of significantly decreasing platelet adhesion as compared to a collagen or stainless steel surface.[227,228]

New stent designs have also incorporated complex arrangements of multiple types of nanoparticles to impart increased functionality and biocompatibility. One method of DES fabrication under investigation is the formation of a multifunctional stent coating created by the layer-by-layer assembly of bioinert biomolecule-based nanoparticles. The nanoparticle layers are formed by spontaneous self-assembly because of alternating electrostatic charges.[229] Using the scalable layer-by-layer assembly method, it is possible to achieve more than 80% stent surface coverage with nanoparticles. A previous study has shown that it is possible to coat a metal stent surface with many different populations of nanoparticles, each of which can be loaded with a different drug. This multifunctional coat can then provide simultaneous, sustained release kinetics of several drugs and can be controlled by altering nanoparticle composition, density, and size, as well as encapsulated drug concentration.[230] The same study also has demonstrated that image contrast agents can be packaged in the same fashion as drugs on a stent surface, resulting in enhancing the quality of imaging by micro computed tomography (using gold nanoparticles) and X-ray (using barium sulfate).

Other studies have produced radio-opaque polymer stents by incorporating poly(ethylene glycol) (PEG) and iodine into the stent, producing X-ray scattering stents capable of decreasing fibrinogen adsorption levels and reducing platelet adhesion to the stent.[231] Furthermore, it has been shown that this technique produces stent images without producing blooming artifacts observed with metal stents.[232]

These complex, multifunctional designs represent a significant advancement in the utilization of nanotechnology for drug eluting stents.

Nanopatterned Surfaces on Bare Metal Stents (BMS)

Many of the negative effects caused by drug eluting stents, such as late stent thrombosis, are because of by-products of stent coating degradation and poor in-stent

endothelialization.[233,234] Occurrence of late stent thrombosis is significantly increased by the use of DES compared to BMS.[200–202] Therefore, as an alternative to DES, advanced BMS attempt to improve stent endothelialization by nanostructuring the stent surface. Introduction of nanoscale surface alterations through patterning or roughening have been shown to improve endothelial cell proliferation and morphology on polymeric and metal materials.[235–238]

Nanopatterned BMS are designed to prevent late stent thrombosis while improving endothelial cell proliferation and retarding smooth muscle cell migration and proliferation. This strategy promotes stent endothelialization and is a promising strategy for preventing restenosis and thrombosis.[239] One group modified a titanium stent surface, creating nanostructured posts with the minimum feature size of $40 \times 40 \times 10$ nm^3 ($l \times w \times h$).[240] They performed a co-culture of rat aorta endothelial cells (RAECs) and rat aorta smooth muscle cells (RASMCs) on the fabricated submicron scale and nanoscale roughed surfaces, with a flat Ti surface serving as a control. RAEC proliferation is increased on roughed Ti surfaces relative to a flat surface even after 1 day and RASMC proliferation is depressed after 5 days. The roughed surfaces exhibited more hydrophilicity as compared to the flat surfaces, improving adsorption of important extracellular matrix proteins such as fibronectin and vitronectin,[241] in addition to increasing RAEC elastin and collagen synthesis after 1 and 2 weeks. Mechanical spreading of RAECs is presumed to increase on roughened surfaces and these morphological changes may account for increased extracellular matrix protein production.[240]

Another group modified the surface of a MP35N alloy (35% Co, 35% Ni, 20% Cr, 10% Mo) stent surface with nanopillars ranging 100–300 nm in diameter and 0.5–5 μm in length.[242] After 2 and 7 days, the textured surfaces showed 50–60% improved bovine aortic endothelial cell adhesion versus a flat stent surface. More importantly, the morphology of the cells on the textured stent surface was comparable to the control cultures and showed the presence of peri-junctional cortical bands of actin filaments indicating physiologically normal arrangement of endothelium. The flat stent surface resulted in poorly organized cellular aggregates exhibiting poorly pronounced cellular junctions and a large amount of poorly organized extracellular matrix protein, indicating the possibility of restenosis[242] (Figure 5).

In addition to the stimulatory mechanical cues presented by the nanopatterned stent surface, the spaces between the nanopillars can potentially be used as depots for drug storage and controlled release as shown with other systems.[243] Drug release kinetics can be controlled by altering the geometric properties of the pillars. BMS modification schemes have also been applied to other stent alloy surfaces such as Ni:Ti alloys and nanoporation of stent surfaces has also been investigated as mechanism of producing surface roughness and drug storage.[244,245]

Nanotechnology based improvements are currently trending toward complex combinatorial approaches designed to inhibit immune response to the implant and prevent restenosis while simultaneously promoting controlled endothelialization using highly biocompatible or bioinert components. To that end, a strong candidate for the next generation of vascular

stents may use a surface modified, nanoroughed BMS surface which in turn contains multiple types of drug eluting and/or contrast enhancing nanoparticles made from biomolecules. This approach would leverage the strengths of the patterned BMS surface while also allowing for localized, sustained drug delivery with highly controllable release kinetics. The implementation of a biomolecular NP drug delivery system would also mitigate the inflammatory and prothrombotic effects of large polymer fragments.

CONCLUSION

Nanotechnology is expected to trigger a revolution in the diagnosis and management of vulnerable plaques. By providing large surface areas for ligand attachment, nanoparticle-based immunoassays and contrast agents are extending the boundaries of sensitivity and detection possible in today's clinic. Further, improvements in nanoparticle design and synthesis continue to produce novel multifunctional platforms, enabling next-generation medical technologies such as multimodal imaging with the same contrast agent, thera-nostic platforms capable of site-specific imaging and therapeutic delivery, multiplexed immunoassays for detecting multiple analytes at once in a single sample, as well as environmentally sensitive 'smart' biosensing. Rapid, low-reagent volume, simple immunoassay setups suggested by the most recent marriages between nanotechnology and microfluidics indicate that routine blood biomarker testing may soon take a more central role in the diagnosis and risk stratification of atherosclerotic patients.

In the cardiac catheterization lab, stenting will continue to be a major means for CAD, and nanotechnology provides a number of unique potential solutions to the most common reasons for stent failure. A long-term goal of the stenting industry is to encourage regeneration of functional endothelium over the stent. Nanopatterning and nanostructuring of stent surfaces creates structures that interact directly with cells on a very relevant size scale, and early studies show promise for this approach to encourage re-endothelialization. Improvements in DES controlled release technologies have also been facilitated through advances in nanoparticle and nanofilm research.

Given the body of promising *in vivo* data in animal models, clinical studies will soon come for these new nanoparticulate diagnostics, contrast agents, controlled-release devices, and stent designs. Next-generation approaches to diagnose and manage vulnerable atherosclerotic plaques are likely to feature nano-based design elements. It is clear that such advances require the concerted efforts of researchers in biomaterials, vascular biology, chemistry, micro-fabrication, and more. These novel approaches are injecting new life into a field, and suggest that a future is coming when vulnerable plaques are detected early and treated accordingly with host-'friendly' stents.

Acknowledgments

S.S.Y., R.A.O., and T.D.G. would like to acknowledge financial support from a Vanderbilt University Discovery Grant (4-48-999-9132) and the Department of Defense Congressionally Directed Medical Research Program (#W81XWH-08-1-0502). H.J.S. acknowledges financial support through the National Institutes of Health (#1R21HL091465) and the National Science Foundation (NSF/DMR BMAT 1006558). S.S.Y. acknowledges his former senior design team members at Rice University—Stacy Cheng, Kai Chu, Shuvro De, Natalia Vasco, & Eva Wang—for providing artwork for Figure 4.

References

1. Lloyd-Jones D, Adams RJ, Brown TM, Carnethon M, Dai S, De Simone G, Ferguson TB, Ford E, Furie K, Gillespie C, et al. Heart disease and stroke statistics—2010 update: a report from the American Heart Association. Circulation. 2010; 121:e46–e215. [PubMed: 20019324]
2. Insull W Jr. The pathology of atherosclerosis: plaque development and plaque responses to medical treatment. Am J Med. 2009; 122:S3–S14.
3. Naghavi, M., Falk, E. Asymptomatic Atherosclerosis. New York, NY: Humana Press; 2010. From vulnerable plaque to vulnerable patient; p. 13-38.
4. Sousa JE, Serruys PW, Costa MA. New frontiers in cardiology: drug-eluting stents: part I. Circulation. 2003; 107:2274–2279. [PubMed: 12732594]
5. Finn AV, Nakazawa G, Joner M, Kolodgie FD, Mont EK, Gold HK, Virmani R. Vascular responses to drug eluting stents: importance of delayed healing. Arterioscler Thromb Vasc Biol. 2007; 27:1500–1510. [PubMed: 17510464]
6. Shyy JY, Chien S. Role of integrins in endothelial mechanosensing of shear stress. Circ Res. 2002; 91:769–775. [PubMed: 12411390]
7. Arroyo LH, Lee RT. Mechanisms of plaque rupture: mechanical and biologic interactions. Cardiovasc Res. 1999; 41:369–375. [PubMed: 10341836]
8. Saam T, Hatsukami TS, Takaya N, Chu B, Under-hill H, Kerwin WS, Cai J, Ferguson MS, Yuan C. The vulnerable, or high-risk, atherosclerotic plaque: non-invasive MR imaging for characterization and assessment. Radiology. 2007; 244:64–77. [PubMed: 17581895]
9. Van Berkel TJ, De Rijke YB, Kruijt JK. Different fate in vivo of oxidatively modified low density lipoprotein and acetylated low density lipoprotein in rats. Recognition by various scavenger receptors on Kupffer and endothelial liver cells. J Biol Chem. 1991; 266:2282–2289. [PubMed: 1989982]
10. Williams KJ, Tabas I. The response-to-retention hypothesis of early atherogenesis. Arterioscler Thromb Vasc Biol. 1995; 15:551–561. [PubMed: 7749869]
11. Tabas I. Consequences and therapeutic implications of macrophage apoptosis in atherosclerosis: the importance of lesion stage and phagocytic efficiency. Arterioscler Thromb Vasc Biol. 2005; 25:2255–2264. [PubMed: 16141399]
12. Pluddemann A, Neyen C, Gordon S. Macrophage scavenger receptors and host-derived ligands. Methods. 2007; 43:207–217. [PubMed: 17920517]
13. Herman MP, Sukhova GK, Libby P, Gerdes N, Tang N, Horton DB, Kilbride M, Breitbart RE, Chun M, Schonbeck U. Expression of neutrophil collagenase (matrix metalloproteinase-8) in human atheroma: a novel collagenolytic pathway suggested by transcriptional profiling. Circulation. 2001; 104:1899–1904. [PubMed: 11602491]
14. Johnson C, Sung HJ, Lessner SM, Fini ME, Galis ZS. Matrix metalloproteinase-9 is required for adequate angiogenic revascularization of ischemic tissues: potential role in capillary branching. Circ Res. 2004; 94:262–268. [PubMed: 14670843]
15. Gough PJ, Gomez IG, Wille PT, Raines EW. Macro-phage expression of active MMP-9 induces acute plaque disruption in apoE-deficient mice. J Clin Invest. 2006; 116:59–69. [PubMed: 16374516]
16. Sluijter JP, Pulskens WP, Schoneveld AH, Velema E, Strijder CF, Moll F, de Vries JP, Verheijen J, Hanemaaijer R, de Kleijn DP, et al. Matrix metal-loproteinase 2 is associated with stable and matrix metalloproteinases 8 and 9 with vulnerable carotid atherosclerotic lesions: a study in human endarterectomy specimen pointing to a role for different extracellular matrix metalloproteinase inducer glycosylation forms. Stroke. 2006; 37:235–239. [PubMed: 16339461]
17. de Nooijer R, Verkleij CJ, von der Thusen JH, Jukema JW, van der Wall EE, van Berkel TJ, Baker AH, Biessen EA. Lesional overexpression of matrix metalloproteinase-9 promotes intraplaque hemorrhage in advanced lesions but not at earlier stages of atherogenesis. Arterioscler Thromb Vasc Biol. 2006; 26:340–346. [PubMed: 16306430]
18. Libby P. Inflammation in atherosclerosis. Nature. 2002; 420:868–874. [PubMed: 12490960]

19. Finet G, Ohayon J, Rioufol G. Biomechanical interaction between cap thickness, lipid core composition and blood pressure in vulnerable coronary plaque: impact on stability or instability. Coron Artery Dis. 2004; 15:13–20. [PubMed: 15201616]
20. Galis ZS, Khatri JJ. Matrix metalloproteinases in vascular remodeling and atherogenesis: the good, the bad, and the ugly. Circ Res. 2002; 90:251–262. [PubMed: 11861412]
21. Galis ZS, Sukhova GK, Lark MW, Libby P. Increased expression of matrix metalloproteinases and matrix degrading activity in vulnerable regions of human atherosclerotic plaques. J Clin Invest. 1994; 94:2493–2503. [PubMed: 7989608]
22. Lee RT, Grodzinsky AJ, Frank EH, Kamm RD, Schoen FJ. Structure-dependent dynamic mechanical behavior of fibrous caps from human atherosclerotic plaques. Circulation. 1991; 83:1764–1770. [PubMed: 2022029]
23. Beaussier H, Masson I, Collin C, Bozec E, Laloux B, Calvet D, Zidi M, Boutouyrie P, Laurent S. Carotid plaque, arterial stiffness gradient, and remodeling in hypertension. Hypertension. 2008; 52:729–736. [PubMed: 18779439]
24. Tajaddini A, Kilpatrick DL, Vince DG. A novel experimental method to estimate stress-strain behavior of intact coronary arteries using intravascular ultrasound (IVUS). J Biomech Eng. 2003; 125:120–123. [PubMed: 12661205]
25. Kim YS, Galis ZS, Rachev A, Han HC, Vito RP. Matrix metalloproteinase-2 and -9 are associated with high stresses predicted using a nonlinear heterogeneous model of arteries. J Biomech Eng. 2009; 131:011009. [PubMed: 19045925]
26. Cheng C, Tempel D, van Haperen R, van der Baan A, Grosveld F, Daemen MJ, Krams R, de Crom R. Atherosclerotic lesion size and vulnerability are determined by patterns of fluid shear stress. Circulation. 2006; 113:2744–2753. [PubMed: 16754802]
27. Douma K, Prinzen L, Slaaf DW, Reutelingsperger CP, Biessen EA, Hackeng TM, Post MJ, van Zand-voort MA. Nanoparticles for optical molecular imaging of atherosclerosis. Small. 2009; 5:544–557. [PubMed: 19226595]
28. Trivedi RA, Mallawarachi C, UK-I JM, Graves MJ, Horsley J, Goddard MJ, Brown A, Wang L, Kirk-patrick PJ, Brown J, et al. Identifying inflamed carotid plaques using in vivo USPIO-enhanced MR imaging to label plaque macrophages. Arterioscler Thromb Vasc Biol. 2006; 26:1601–1606. [PubMed: 16627809]
29. Holzapfel GA, Sommer G, Regitnig P. Anisotropic mechanical properties of tissue components in human atherosclerotic plaques. J Biomech Eng. 2004; 126:657–665. [PubMed: 15648819]
30. Richardson PD. Biomechanics of plaque rupture: progress, problems, and new frontiers. Ann Biomed Eng. 2002; 30:524–536. [PubMed: 12086003]
31. Little WC, Constantinescu M, Applegate RJ, Kutcher MA, Burrows MT, Kahl FR, Santamore WP. Can coronary angiography predict the site of a subsequent myocardial infarction in patients with mild-to-moderate coronary artery disease? Circulation. 1988; 78:1157–1166. [PubMed: 3180375]
32. Giroud D, Li JM, Urban P, Meier B, Rutishauer W. Relation of the site of acute myocardial infarction to the most severe coronary arterial stenosis at prior angiography. Am J Cardiol. 1992; 69:729–732. [PubMed: 1546645]
33. Cutlip DE, Chhabra AG, Baim DS, Chauhan MS, Marulkar S, Massaro J, Bakhai A, Cohen DJ, Kuntz RE, Ho KK. Beyond restenosis: five-year clinical outcomes from second-generation coronary stent trials. Circulation. 2004; 110:1226–1230. [PubMed: 15337693]
34. Glaser R, Selzer F, Faxon DP, Laskey WK, Cohen HA, Slater J, Detre KM, Wilensky RL. Clinical progression of incidental, asymptomatic lesions discovered during culprit vessel coronary intervention. Circulation. 2005; 111:143–149. [PubMed: 15623544]
35. de Weert TT, Ouhlous M, Meijering E, Zondervan PE, Hendriks JM, van Sambeek MR, Dippel DW, van der Lugt A. In vivo characterization and quantification of atherosclerotic carotid plaque components with multidetector computed tomography and histopathological correlation. Arterioscler Thromb Vasc Biol. 2006; 26:2366–2372. [PubMed: 16902158]
36. Das M, Braunschweig T, Muhlenbruch G, Mahnken AH, Krings T, Langer S, Koeppel T, Jacobs M, Gunther RW, Mommertz G. Carotid plaque analysis: comparison of dual-source computed tomography (CT) findings and histopathological correlation. Eur J Vasc Endovasc Surg. 2009; 38:14–19. [PubMed: 19464932]

37. Cai J, Hatsukami TS, Ferguson MS, Kerwin WS, Saam T, Chu B, Takaya N, Polissar NL, Yuan C. In vivo quantitative measurement of intact fibrous cap and lipid-rich necrotic core size in atherosclerotic carotid plaque: comparison of high-resolution, contrast-enhanced magnetic resonance imaging and histology. Circulation. 2005; 112:3437–3444. [PubMed: 16301346]
38. Beduneau A, Ma Z, Grotepas CB, Kabanov A, Rabinow BE, Gong N, Mosley RL, Dou H, Boska MD, Gendelman HE. Facilitated monocyte-macrophage uptake and tissue distribution of superparmagnetic iron-oxide nanoparticles. PLoS One. 2009; 4:e4343. [PubMed: 19183814]
39. Briley-Saebo KC, Johansson LO, Hustvedt SO, Haldorsen AG, Bjornerud A, Fayad ZA, Ahlstrom HK. Clearance of iron oxide particles in rat liver—effect of hydrated particle size and coating material on liver metabolism. Invest Radiol. 2006; 41:560–571. [PubMed: 16772849]
40. Briley-Saebo KC, Mani V, Hyafil F, Cornily JC, Fayad ZA. Fractionated feridex and positive contrast: in vivo MR imaging of atherosclerosis. Magn Reson Med. 2008; 59:721–730. [PubMed: 18383304]
41. Tang TY, Muller KH, Graves MJ, Li ZY, Walsh SR, Young V, Sadat U, Howarth SP, Gillard JH. Iron oxide particles for atheroma imaging. Arterioscler Thromb Vasc Biol. 2009; 29:1001–1008. [PubMed: 19229073]
42. Thomsen HS. Gadolinium-based contrast media may be nephrotoxic even at approved doses. Eur Radiol. 2004; 14:1654–1656. [PubMed: 15221265]
43. Bastus NG, Sanchez-Tillo E, Pujals S, Farrera C, Lopez C, Giralt E, Celada A, Lloberas J, Puntes V. Homogeneous conjugation of peptides onto gold nanoparticles enhances macrophage response. ACS Nano. 2009; 3:1335–1344. [PubMed: 19489561]
44. Simberg D, Park JH, Karmali PP, Zhang WM, Merkulov S, McCrae K, Bhatia SN, Sailor M, Ruoslahti E. Differential proteomics analysis of the surface heterogeneity of dextran iron oxide nanoparticles and the implications for their in vivo clearance. Biomaterials. 2009; 30:3926–3933. [PubMed: 19394687]
45. Fujimoto S, Hartung D, Ohshima S, Edwards DS, Zhou J, Yalamanchili P, Azure M, Fujimoto A, Isobe S, Matsumoto Y, et al. Molecular imaging of matrix metalloproteinase in atherosclerotic lesions: resolution with dietary modification and statin therapy. J Am Coll Cardiol. 2008; 52:1847–1857. [PubMed: 19038682]
46. Kooi ME, Cappendijk VC, Cleutjens KB, Kessels AG, Kitslaar PJ, Borgers M, Frederik PM, Daemen MJ, van Engelshoven JM. Accumulation of ultrasmall superparamagnetic particles of iron oxide in human atherosclerotic plaques can be detected by in vivo magnetic resonance imaging. Circulation. 2003; 107:2453–2458. [PubMed: 12719280]
47. Lipinski MJ, Frias JC, Amirbekian V, Briley-Saebo KC, Mani V, Samber D, Abbate A, Aguinaldo JG, Massey D, Fuster V, et al. Macrophage-specific lipid-based nanoparticles improve cardiac magnetic resonance detection and characterization of human atherosclerosis. JACC Cardiovasc Imaging. 2009; 2:637–647. [PubMed: 19442953]
48. Nahrendorf M, Zhang H, Hembrador S, Panizzi P, Sosnovik DE, Aikawa E, Libby P, Swirski FK, Weissleder R. Nanoparticle PET-CT imaging of macrophages in inflammatory atherosclerosis. Circulation. 2008; 117:379–387. [PubMed: 18158358]
49. Trivedi RA, UK-I JM, Graves MJ, Kirkpatrick PJ, Gillard JH. Noninvasive imaging of carotid plaque inflammation. Neurology. 2004; 63:187–188. [PubMed: 15249641]
50. Waldo SW, Li Y, Buono C, Zhao B, Billings EM, Chang J, Kruth HS. Heterogeneity of human macrophages in culture and in atherosclerotic plaques. Am J Pathol. 2008; 172:1112–1126. [PubMed: 18321997]
51. Raynal I, Prigent P, Peyramaure S, Najid A, Rebuzzi C, Corot C. Macrophage endocytosis of super-paramagnetic iron oxide nanoparticles: mechanisms and comparison of ferumoxides and ferumoxtran-10. Invest Radiol. 2004; 39:56–63. [PubMed: 14701989]
52. Sanz J, Fayad ZA. Imaging of atherosclerotic cardiovascular disease. Nature. 2008; 451:953–957. [PubMed: 18288186]
53. Moreno PR, Purushothaman KR, Fuster V, Echeverri D, Truszczynska H, Sharma SK, Badimon JJ, O'Connor WN. Plaque neovascularization is increased in ruptured atherosclerotic lesions of human aorta: implications for plaque vulnerability. Circulation. 2004; 110:2032–2038. [PubMed: 15451780]

54. Giannarelli C, Ibanez B, Cimmino G, Garcia Ruiz JM, Faita F, Bianchini E, Zafar MU, Fuster V, Garcia MJ, Badimon JJ. Contrast-enhanced ultrasound imaging detects intraplaque neovascularization in an experimental model of atherosclerosis. JACC Cardiovasc Imaging. 2010; 3:1256–1264. [PubMed: 21163454]
55. Manca C, Parenti G, Bellina R, Boni G, Grosso M, Bernini W, Palombo C, Paterni M, Pelosi G, Lanza M, et al. In-111 platelet scintigraphy for the noninvasive detection of carotid plaque thrombosis. Stroke. 2001; 32:719–727. [PubMed: 11239193]
56. Annovazzi A, Bonanno E, Arca M, D'Alessandria C, Marcoccia A, Spagnoli LG, Violi F, Scopinaro F, De Toma G, Signore A. 99mTc-interleukin-2 scintigraphy for the in vivo imaging of vulnerable atherosclerotic plaques. Eur J Nucl Med Mol Imaging. 2006; 33:117–126. [PubMed: 16220305]
57. Tawakol A, Migrino RQ, Bashian GG, Bedri S, Vermylen D, Cury RC, Yates D, LaMuraglia GM, Furie K, Houser S, et al. In vivo 18F-fluorode-oxyglucose positron emission tomography imaging provides a noninvasive measure of carotid plaque inflammation in patients. J Am Coll Cardiol. 2006; 48:1818–1824. [PubMed: 17084256]
58. Burke AP, Farb A, Malcom GT, Liang YH, Smialek J, Virmani R. Coronary risk factors and plaque morphology in men with coronary disease who died suddenly. N Engl J Med. 1997; 336:1276–1282. [PubMed: 9113930]
59. Yamagishi M, Terashima M, Awano K, Kijima M, Nakatani S, Daikoku S, Ito K, Yasumura Y, Miyatake K. Morphology of vulnerable coronary plaque: insights from follow-up of patients examined by intravascular ultrasound before an acute coronary syndrome. J Am Coll Cardiol. 2000; 35:106–111. [PubMed: 10636267]
60. Bayturan O, Tuzcu EM, Nicholls SJ, Balog C, Lavoie A, Uno K, Crowe TD, Magyar WA, Wolski K, Kapadia S, et al. Attenuated plaque at nonculprit lesions in patients enrolled in intravascular ultrasound atherosclerosis progression trials. JACC Cardiovasc Interv. 2009; 2:672–678. [PubMed: 19628192]
61. Lee SY, Mintz GS, Kim SY, Hong YJ, Kim SW, Okabe T, Pichard AD, Satler LF, Kent KM, Suddath WO, et al. Attenuated plaquedetected byintravascular ultrasound: clinical, angiographic, and morphologic features and post-percutaneous coronary intervention complications in patients with acute coronary syndromes. JACC Cardiovasc Interv. 2009; 2:65–72. [PubMed: 19463400]
62. Nair A, Kuban BD, Tuzcu EM, Schoenhagen P, Nissen SE, Vince DG. Coronary plaque classification with intravascular ultrasound radiofrequency data analysis. Circulation. 2002; 106:2200–2206. [PubMed: 12390948]
63. Van Herck J, De Meyer G, Ennekens G, Van Herck P, Herman A, Vrints C. Validation of in vivo plaque characterisation by virtual histology in a rabbit model of atherosclerosis. EuroIntervention. 2009; 5:149–156. [PubMed: 19577997]
64. Rodriguez-Granillo GA, Garcia-Garcia HM, Mc Fadden EP, Valgimigli M, Aoki J, de Feyter P, Serruys PW. In vivo intravascular ultrasound-derived thin-cap fibroatheroma detection using ultrasound radiofrequency data analysis. J Am Coll Cardiol. 2005; 46:2038–2042. [PubMed: 16325038]
65. Serruys PW. Fourth annual American College of Cardiology international lecture: a journey in the interventional field. J Am Coll Cardiol. 2006; 47:1754–1768. [PubMed: 16682299]
66. Stone GW, Maehara A, Lansky AJ, de Bruyne B, Cristea E, Mintz GS, Mehran R, McPherson J, Farhat N, Marso SP, et al. A prospective natural-history study of coronary atherosclerosis. New Engl J Med. 2011; 364:226–235. [PubMed: 21247313]
67. Low AF, Tearney GJ, Bouma BE, Jang IK. Technology Insight: optical coherence tomography-current status and future development. Nat Clin Pract Cardiovasc Med. 2006; 3:154–162. quiz 172. [PubMed: 16505861]
68. Stamper D, Weissman NJ, Brezinski M. Plaque characterization with optical coherence tomography. J Am Coll Cardiol. 2006; 47:C69–C79. [PubMed: 16631512]
69. Templin C, Meyer M, Muller MF, Djonov V, Hlushchuk R, Dimova I, Flueckiger S, Kronen P, Sidler M, Klein K, et al. Coronary optical frequency domain imaging (OFDI) for in vivo evaluation of stent healing: comparison with light and electron microscopy. Eur Heart J. 2010; 31:1792–1801. [PubMed: 20525979]

70. Fuster V, Fayad ZA, Moreno PR, Poon M, Corti R, Badimon JJ. Atherothrombosis and high-risk plaque: Part II: approaches by noninvasive computed tomo-graphic/magnetic resonance imaging. J Am Coll Cardiol. 2005; 46:1209–1218. [PubMed: 16198833]
71. Fuster V, Corti R, Fayad ZA, Schwitter J, Badimon JJ. Integration of vascular biology and magnetic resonance imaging in the understanding of atherothrombosis and acute coronary syndromes. J Thromb Haemost. 2003; 1:1410–1421. [PubMed: 12871275]
72. Sirol M, Fuster V, Fayad ZA. Plaque imaging and characterization using magnetic resonance imaging: towards molecular assessment. Curr Mol Med. 2006; 6:541–548. [PubMed: 16918374]
73. Moreno PR. Vulnerable plaque: definition, diagnosis, and treatment. Cardiol Clin. 2010; 28:1–30. [PubMed: 19962047]
74. Sathyanarayana S, Schar M, Kraitchman DL, Bottomley PA. Towards real-time intravascular endoscopic magnetic resonance imaging. JACC Cardiovasc Imaging. 2010; 3:1158–1165. [PubMed: 21071004]
75. Hirsch LR, Stafford RJ, Bankson JA, Sershen SR, Rivera B, Price RE, Hazle JD, Halas NJ, West JL. Nanoshell-mediated near-infrared thermal therapy of tumors under magnetic resonance guidance. Proc Natl Acad Sci USA. 2003; 100:13549–13554. [PubMed: 14597719]
76. Luker GD, Luker KE. Optical imaging: current applications and future directions. J Nucl Med. 2008; 49:1–4. [PubMed: 18077528]
77. Goldstein JA, Grines C, Fischell T, Virmani R, Rizik D, Muller J, Dixon SR. Coronary embolization following balloon dilation of lipid-core plaques. JACC Cardiovasc imaging. 2009; 2:1420–1424. [PubMed: 20083078]
78. Madden, SP., Sum, ST., Muller, JE. Assessment of coronary stenosis with near infrared spectroscopy. In: Escaned, J., Serruys, P., editors. Coronary Stenosis Imaging, Structure, and Physiology. Toulouse: PCR Publishing; 2010.
79. Caplan JD, Waxman S, Nesto RW, Muller JE. Near-infrared spectroscopy for the detection of vulnerable coronary artery plaques. J Am Coll Cardiol. 2006; 47:C92–C96. [PubMed: 16631516]
80. Gardner CM, Tan H, Hull EL, Lisauskas JB, Sum ST, Meese TM, Jiang C, Madden SP, Caplan JD, Burke AP, et al. Detection of lipid core coronary plaques in autopsy specimens with a novel catheter-based near-infrared spectroscopy system. JACC Cardiovasc Imaging. 2008; 1:638–648. [PubMed: 19356494]
81. Moreno PR, Lodder RA, Purushothaman KR, Charash WE, O'Connor WN, Muller JE. Detection of lipid pool, thin fibrous cap, and inflammatory cells in human aortic atherosclerotic plaques by near-infrared spectroscopy. Circulation. 2002; 105:923–927. [PubMed: 11864919]
82. Schultz CJ, Serruys PW, van der Ent M, Ligthart J, Mastik F, Garg S, Muller JE, Wilder MA, van de Steen AFW, Regar E. First-in-man clinical use of combined near-infrared spectroscopy and intravascular ultrasound a potential key to predict distal embolization and no-reflow? J Am Coll Cardiol. 2010; 56:314–314. [PubMed: 20633824]
83. Libby P, Aikawa M. Stabilization of atherosclerotic plaques: new mechanisms and clinical targets. Nat Med. 2002; 8:1257–1262. [PubMed: 12411953]
84. Jaffer FA, Libby P, Weissleder R. Molecular and cellular imaging of atherosclerosis: emerging applications. J Am Coll Cardiol. 2006; 47:1328–1338. [PubMed: 16580517]
85. Ni M, Chen WQ, Zhang Y. Animal models and potential mechanisms of plaque destabilisation and disruption. Heart. 2009; 95:1393–1398. [PubMed: 19153105]
86. Nahrendorf M, Waterman P, Thurber G, Groves K, Rajopadhye M, Panizzi P, Marinelli B, Aikawa E, Pittet MJ, Swirski FK, et al. Hybrid in vivo FMT-CT imaging of protease activity in atherosclerosis with customized nanosensors. Arterioscler Thromb Vasc Biol. 2009; 29:1444–1451. [PubMed: 19608968]
87. Ma LL, Feldman MD, Tam JM, Paranjape AS, Cheruku KK, Larson TA, Tam JO, Ingram DR, Paramita V, Villard JW, et al. Small multifunctional nanoclusters (nanoroses) for targeted cellular imaging and therapy. ACS Nano. 2009; 3:2686–2696. [PubMed: 19711944]
88. Kang HW, Josephson L, Petrovsky A, Weissleder R, Bogdanov A Jr. Magnetic resonance imaging of inducible E-selectin expression in human endothelial cell culture. Bioconjug Chem. 2002; 13:122–127. [PubMed: 11792187]

89. Kang HW, Torres D, Wald L, Weissleder R, Bogdanov AA Jr. Targeted imaging of human endothelial-specific marker in a model of adoptive cell transfer. Lab Invest. 2006; 86:599–609. [PubMed: 16607378]

90. Flacke S, Fischer S, Scott MJ, Fuhrhop RJ, Allen JS, McLean M, Winter P, Sicard GA, Gaffney PJ, Wickline SA, et al. Novel MRI contrast agent for molecular imaging of fibrin: implications for detecting vulnerable plaques. Circulation. 2001; 104:1280–1285. [PubMed: 11551880]

91. Peters D, Kastantin M, Kotamraju VR, Karmali PP, Gujraty K, Tirrell M, Ruoslahti E. Targeting atherosclerosis by using modular, multifunctional micelles. Proc Natl Acad Sci U S A. 2009; 106:9815–9819. [PubMed: 19487682]

92. Cormode DP, Briley-Saebo KC, Mulder WJ, Aguinaldo JG, Barazza A, Ma Y, Fisher EA, Fayad ZA. An ApoA-I mimetic peptide high-density-lipoprotein-based MRI contrast agent for atherosclerotic plaque composition detection. Small. 2008; 4:1437–1444. [PubMed: 18712752]

93. Cormode DP, Roessl E, Thran A, Skajaa T, Gordon RE, Schlomka JP, Fuster V, Fisher EA, Mulder WJ, Proksa R, et al. Atherosclerotic plaque composition: analysis with multicolor CT and targeted gold nanoparticles. Radiology. 2010; 256:774–782. [PubMed: 20668118]

94. Frias JC, Williams KJ, Fisher EA, Fayad ZA. Recombinant HDL-like nanoparticles: a specific contrast agent for MRI of atherosclerotic plaques. J Am Chem Soc. 2004; 126:16316–16317. [PubMed: 15600321]

95. Cormode DP, Skajaa T, van Schooneveld MM, Koole R, Jarzyna P, Lobatto ME, Calcagno C, Barazza A, Gordon RE, Zanzonico P, et al. Nanocrystal core high-density lipoproteins: a multimodality contrast agent platform. Nano Lett. 2008; 8:3715–3723. [PubMed: 18939808]

96. Tang TY, Howarth SP, Miller SR, Graves MJ, Patterson AJ, UK-I JM, Li ZY, Walsh SR, Brown AP, Kirkpatrick PJ, et al. The ATHEROMA (Atorvastatin Therapy: Effects on Reduction of Macrophage Activity) Study. Evaluation using ultrasmall superpara-magnetic iron oxide-enhanced magnetic resonance imaging in carotid disease. J Am Coll Cardiol. 2009; 53:2039–2050. [PubMed: 19477353]

97. Morishige K, Kacher DF, Libby P, Josephson L, Ganz P, Weissleder R, Aikawa M. High-resolution magnetic resonance imaging enhanced with superpara-magnetic nanoparticles measures macrophage burden in atherosclerosis. Circulation. 2010; 122:1707–1715. [PubMed: 20937980]

98. Wang B, Yantsen E, Larson T, Karpiouk AB, Sethuraman S, Su JL, Sokolov K, Emelianov SY. Plasmonic intravascular photoacoustic imaging for detection of macrophages in atherosclerotic plaques. Nano Lett. 2009; 9:2212–2217. [PubMed: 18844426]

99. Hyafil F, Cornily JC, Feig JE, Gordon R, Vucic E, Amirbekian V, Fisher EA, Fuster V, Feldman LJ, Fayad ZA. Noninvasive detection of macrophages using a nanoparticulate contrast agent for computed tomography. Nat Med. 2007; 13:636–641. [PubMed: 17417649]

100. Hyafil F, Cornily JC, Rudd JH, Machac J, Feldman LJ, Fayad ZA. Quantification of inflammation within rabbit atherosclerotic plaques using the macrophage-specific CT contrast agent N1177: a comparison with 18F-FDG PET/CT and histology. J Nucl Med. 2009; 50:959–965. [PubMed: 19443582]

101. Harris TJ, von Maltzahn G, Lord ME, Park JH, Agrawal A, Min DH, Sailor MJ, Bhatia SN. Protease-triggered unveiling of bioactive nanoparticles. Small. 2008; 4:1307–1312. [PubMed: 18690639]

102. Schellenberger E, Rudloff F, Warmuth C, Taupitz M, Hamm B, Schnorr J. Protease-specific nanosensors for magnetic resonance imaging. Bioconjug Chem. 2008; 19:2440–2445. [PubMed: 19007261]

103. Briley-Saebo KC, Shaw PX, Mulder WJ, Choi SH, Vucic E, Aguinaldo JG, Witztum JL, Fuster V, Tsimikas S, Fayad ZA. Targeted molecular probes for imaging atherosclerotic lesions with magnetic resonance using antibodies that recognize oxidation-specific epitopes. Circulation. 2008; 117:3206–3215. [PubMed: 18541740]

104. Briley-Saebo KC, Cho YS, Shaw PX, Ryu SK, Mani V, Dickson S, Izadmehr E, Green S, Fayad ZA, Tsimikas S. Targeted iron oxide particles for in vivo magnetic resonance detection of atherosclerotic lesions with antibodies directed to oxidation-specific epitopes. J Am Coll Cardiol. 2011; 57:337–347. [PubMed: 21106318]

105. van Tilborg GA, Vucic E, Strijkers GJ, Cormode DP, Mani V, Skajaa T, Reutelingsperger CP, Fayad ZA, Mulder WJ, Nicolay K. Annexin A5-functionalized bimodal nanoparticles for MRI and fluorescence imaging of atherosclerotic plaques. Bioconjug Chem. 2010; 21:1794–1803. [PubMed: 20804153]
106. Lee D, Khaja S, Velasquez-Castano JC, Dasari M, Sun C, Petros J, Taylor WR, Murthy N. In vivo imaging of hydrogen peroxide with chemiluminescent nanoparticles. Nat Mater. 2007; 6:765–769. [PubMed: 17704780]
107. Lipinski MJ, Amirbekian V, Frias JC, Aguinaldo JG, Mani V, Briley-Saebo KC, Fuster V, Fallon JT, Fisher EA, Fayad ZA. MRI to detect atherosclerosis with gadolinium-containing immunomicelles targeting the macrophage scavenger receptor. Magn Reson Med. 2006; 56:601–610. [PubMed: 16902977]
108. Amirbekian V, Lipinski MJ, Briley-Saebo KC, Amirbekian S, Aguinaldo JG, Weinreb DB, Vucic E, Frias JC, Hyafil F, Mani V, et al. Detecting and assessing macrophages in vivo to evaluate atherosclerosis non-invasively using molecular MRI. Proc Natl Acad Sci USA. 2007; 104:961–966. [PubMed: 17215360]
109. Nahrendorf M, Jaffer FA, Kelly KA, Sosnovik DE, Aikawa E, Libby P, Weissleder R. Noninvasive vascular cell adhesion molecule-1 imaging identifies inflammatory activation of cells in atherosclerosis. Circulation. 2006; 114:1504–1511. [PubMed: 17000904]
110. Tsourkas A, Shinde-Patil VR, Kelly KA, Patel P, Wolley A, Allport JR, Weissleder R. In vivo imaging of activated endothelium using an anti-VCAM-1 magne-tooptical probe. Bioconjug Chem. 2005; 16:576–581. [PubMed: 15898724]
111. Kelly KA, Allport JR, Tsourkas A, Shinde-Patil VR, Josephson L, Weissleder R. Detection of vascular adhesion molecule-1 expression using a novel multimodal nanoparticle. Circ Res. 2005; 96:327–336. [PubMed: 15653572]
112. Winter PM, Morawski AM, Caruthers SD, Fuhrhop RW, Zhang H, Williams TA, Allen JS, Lacy EK, Robertson JD, Lanza GM, et al. Molecular imaging of angiogenesis in early-stage atherosclerosis with α(v)β3-integrin-targeted nanoparticles. Circulation. 2003; 108:2270–2274. [PubMed: 14557370]
113. Tomokiyo R, Jinnouchi K, Honda M, Wada Y, Hanada N, Hiraoka T, Suzuki H, Kodama T, Takahashi K, Takeya M. Production, characterization, and interspecies reactivities of monoclonal antibodies against human class A macrophage scavenger receptors. Atherosclerosis. 2002; 161:123–132. [PubMed: 11882324]
114. Guray U, Erbay AR, Guray Y, Yilmaz MB, Boyaci AA, Sasmaz H, Korkmaz S, Kutuk E. Levels of soluble adhesion molecules in various clinical presentations of coronaryatherosclerosis. Int J Cardiol. 2004; 96:235–240. [PubMed: 15262039]
115. de Boer OJ, van der Wal AC, Teeling P, Becker AE. Leucocyte recruitment in rupture prone regions of lipid-rich plaques: a prominent role for neovascularization? Cardiovasc Res. 1999; 41:443–449. [PubMed: 10341843]
116. Brown MS, Goldstein JL. Lipoprotein metabolism in the macrophage: implications for cholesterol deposition in atherosclerosis. Annu Rev Biochem. 1983; 52:223–261. [PubMed: 6311077]
117. Nagaoka K, Takahara K, Tanaka K, Yoshida H, Steinman RM, Saitoh S, Akashi-Takamura S, Miyake K, Kang YS, Park CG, et al. Association of SIGNR1 with TLR4-MD-2 enhances signal transduction by recognition of LPS in gram-negative bacteria. Int Immunol. 2005; 17:827–836. [PubMed: 15908446]
118. Mulder WJ, Strijkers GJ, Briley-Saboe KC, Frias JC, Aguinaldo JG, Vucic E, Amirbekian V, Tang C, Chin PT, Nicolay K, et al. Molecular imaging of macrophages in atherosclerotic plaques using bimodal PEG-micelles. Magn Reson Med. 2007; 58:1164–1170. [PubMed: 18046703]
119. Tsimikas S, Mallat Z, Talmud PJ, Kastelein JJP, Wareham NJ, Sandhu MS, Miller ER, Benessiano J, Tedgui A, Witztum JL, et al. Oxidation-Specific Biomarkers, Lipoprotein(a), and Risk of Fatal and Nonfatal Coronary Events. J Am Coll Cardiol. 2010; 56:946–955. [PubMed: 20828647]
120. Woo K, Hong J, Choi S, Lee HW, Ahn JP, Kim CS, Lee SW. Easy synthesis and magnetic properties of iron oxide nanoparticles. Chem Mater. 2004; 16:2814–2818.

121. Dubertret B, Skourides P, Norris DJ, Noireaux V, Brivanlou AH, Libchaber A. In vivo imaging of quantum dots encapsulated in phospholipid micelles. Science. 2002; 298:1759–1762. [PubMed: 12459582]
122. Park J, Joo J, Kwon SG, Jang Y, Hyeon T. Synthesis of monodisperse spherical nanocrystals. Angew Chem Int Ed. 2007; 46:4630–4660.
123. Kelly KA, Nahrendorf M, Yu AM, Reynolds F, Weissleder R. In vivo phage display selection yields atherosclerotic plaque targeted peptides for imaging. Mol Imaging Biol. 2006; 8:201–207. [PubMed: 16791746]
124. Paranjape AS, Kuranov R, Baranov S, Ma LL, Villard JW, Wang T, Sokolov KV, Feldman MD, Johnston KP, Milner TE. Depth resolved photothermal OCT detection of macrophages in tissue using nanorose. Biomed Opt Exp. 2010; 1:2–16.
125. Yu SS, Scherer RL, Ortega RA, Bell CS, O'Neil CP, Hubbell JA, Giorgio TD. Enzymatic- and temperature-sensitive controlled release of ultrasmall superpara-magnetic iron oxides (USPIOs). J Nanobiotechnol. 2011; 9:7.
126. Beumer JH, Boisdron-Celle M, Clarke W, Courtney JB, Egorin MJ, Gamelin E, Harney RL, Hammett-Stabler C, Lepp S, Li Y, et al. Multicenter evaluation of a novel nanoparticle immunoassay for 5-fluorouracil on the Olympus AU400 analyzer. Ther Drug Monit. 2009; 31:688–694. [PubMed: 19935361]
127. Jaffer FA, Kim DE, Quinti L, Tung CH, Aikawa E, Pande AN, Kohler RH, Shi GP, Libby P, Weissleder R. Optical visualization of cathepsin K activity in atherosclerosis with a novel, protease-activatable fluorescence sensor. Circulation. 2007; 115:2292–2298. [PubMed: 17420353]
128. Sukhova GK, Shi GP, Simon DI, Chapman HA, Libby P. Expression of the elastolytic cathepsins S and K in human atheroma and regulation of their production in smooth muscle cells. J Clin Invest. 1998; 102:576–583. [PubMed: 9691094]
129. Rodgers KJ, Watkins DJ, Miller AL, Chan PY, Karanam S, Brissette WH, Long CJ, Jackson CL. Destabilizing role of cathepsin S in murine atherosclerotic plaques. Arterioscler Thromb Vasc Biol. 2006; 26:851–856. [PubMed: 16410454]
130. Li W, Yuan XM. Increased expression and translocation of lysosomal cathepsins contribute to macrophage apoptosis in atherogenesis. Ann N Y Acad Sci. 2004; 1030:427–433. [PubMed: 15659826]
131. Tung CH, Bredow S, Mahmood U, Weissleder R. Preparation of a cathepsin D sensitive near-infrared fluorescence probe for imaging. Bioconjug Chem. 1999; 10:892–896. [PubMed: 10502358]
132. Lakowicz, JR. Principles of Fluorescence Spectroscopy. 3rd. New York: Springer; 2006.
133. Deguchi JO, Aikawa M, Tung CH, Aikawa E, Kim DE, Ntziachristos V, Weissleder R, Libby P. Inflammation in atherosclerosis: visualizing matrix metallo-proteinase action in macrophages in vivo. Circulation. 2006; 114:55–62. [PubMed: 16801460]
134. Chen J, Tung CH, Mahmood U, Ntziachristos V, Gyurko R, Fishman MC, Huang PL, Weissleder R. In vivo imaging of proteolytic activity in atherosclerosis. Circulation. 2002; 105:2766–2771. [PubMed: 12057992]
135. Altinoglu EI, Adair JH. Near infrared imaging with nanoparticles. Wiley Interdiscip Rev Nanomed Nanobiotechnol. 2010; 2:461–477. [PubMed: 20135691]
136. Chang E, Miller JS, Sun J, Yu WW, Colvin VL, Drezek R, West JL. Protease-activated quantum dot probes. Biochem Biophys Res Commun. 2005; 334:1317–1321. [PubMed: 16039606]
137. Sun J, Fu K, Zhu M-Q, Bickford L, Post E, Drezek R. Near-infrared quantum dot contrast agents for fluorescence tissue imaging: a phantom study. Curr Nanosci. 2009; 5:160–166.
138. Smith AM, Nie S. Bright and compact alloyed quantum dots with broadly tunable near-infrared absorption and fluorescence spectra through mercury cation exchange. J Am Chem Soc. 2010; 133:24–26. [PubMed: 21142154]
139. Ma Q, Su X. Near-infrared quantum dots: synthesis, functionalization and analytical applications. Analyst. 2010; 135:1867–1877. [PubMed: 20563343]

140. Kim S, Lim YT, Soltesz EG, De Grand AM, Lee J, Nakayama A, Parker JA, Mihaljevic T, Laurence RG, Dor DM, et al. Near-infrared fluorescent type II quantum dots for sentinel lymph node mapping. Nat Biotechnol. 2004; 22:93–97. [PubMed: 14661026]
141. Bailey RE, Strausburg JB, Nie S. A new class of far-red and near-infrared biological labels based on alloyed semiconductor quantum dots. J Nanosci Nanotechnol. 2004; 4:569–574. [PubMed: 15518388]
142. Hauck TS, Anderson RE, Fischer HC, Newbigging S, Chan WC. In vivo quantum-dot toxicity assessment. Small. 2010; 6:138–144. [PubMed: 19743433]
143. Chang E, Thekkek N, Yu WW, Colvin VL, Drezek R. Evaluation of quantum dot cytotoxicity based on intra-cellular uptake. Small. 2006; 2:1412–1417. [PubMed: 17192996]
144. Sewell SL, Giorgio TD. Synthesis and enzymatic cleavage of dual-ligand quantum dots. Mater Sci Eng C Mater Biol Appl. 2009; 29:1428–1432.
145. Smith R, Sewell SL, Giorgio TD. Proximity-activated nanoparticles: in vitro performance of specific structural modification by enzymatic cleavage. Int J Nanomed. 2008; 3:95–103.
146. Sewell SL, Giorgio TD. Surface functionalized nano-particles for proximity-activated detection and imaging of breast cancer. Cancer Res. 2009; 69:348s.
147. Guyton, AC., Hall, JE. Textbook of Medical Physiology. 11th. Philadelphia: Elsevier Saunders; 2006.
148. Brannon-Peppas L, Blanchette JO. Nanoparticle and targeted systems for cancer therapy. Adv Drug Deliv Rev. 2004; 56:1649–1659. [PubMed: 15350294]
149. Storm G, Belliot SO, Daemen T, Lasic DD. Surface modification of nanoparticles to oppose uptake by the mononuclear phagocyte system. Adv Drug Delivery Rev. 1995; 17:31–48.
150. Li SD, Huang L. Nanoparticles evading the reticuloendothelial system: role of the supported bilayer. Biochim Biophys Acta. 2009; 1788:2259–2266. [PubMed: 19595666]
151. Kirkland-York S, Zhang Y, Smith AE, York AW, Huang F, McCormick CL. Tailored design of Au nanoparticle-siRNA carriers utilizing reversible addition-fragmentation chain transfer polymers. Biomacromolecules. 2010; 11:1052–1059. [PubMed: 20337403]
152. Wickline SA, Neubauer AM, Winter PM, Caruthers SD, Lanza GM. Molecular imaging and therapy of atherosclerosis with targeted nanoparticles. J Magn Reson Imaging. 2007; 25:667–680. [PubMed: 17347992]
153. Maeda H, Wu J, Sawa T, Matsumura Y, Hori K. Tumor vascular permeability and the EPR effect in macromolecular therapeutics: a review. J Contr Rel. 2000; 65:271–284.
154. Davis ME, Zuckerman JE, Choi CH, Seligson D, Tolcher A, Alabi CA, Yen Y, Heidel JD, Ribas A. Evidence of RNAi in humans from systemically administered siRNA via targeted nanoparticles. Nature. 2010; 464:1067–1070. [PubMed: 20305636]
155. Weissleder R, Kelly K, Sun EY, Shtatland T, Josephson L. Cell-specific targeting of nanoparticles by multi-valent attachment of small molecules. Nat Biotechnol. 2005; 23:1418–1423. [PubMed: 16244656]
156. Senpan A, Caruthers SD, Rhee I, Mauro NA, Pan D, Hu G, Scott MJ, Fuhrhop RW, Gaffney PJ, Wickline SA, et al. Conquering the dark side: colloidal iron oxide nanoparticles. Acs Nano. 2009; 3:3917–3926. [PubMed: 19908850]
157. Erogbogbo F, Yong K-T, Roy I, Xu G, Prasad PN, Swihart MT. Biocompatible luminescent silicon quantum dots for imaging of cancer cells. Acs Nano. 2008; 2:873–878. [PubMed: 19206483]
158. McIntyre JO, Scherer RL, Matrisian LM. Near-infrared optical proteolytic beacons for in vivo imaging of matrix metalloproteinase activity. Methods Mol Biol. 2010; 622:279–304. [PubMed: 20135290]
159. Scherer RL, VanSaun MN, McIntyre JO, Matrisian LM. Optical imaging of matrix metalloproteinase-7 activity in vivo using a proteolytic nanobeacon. Mol Imaging. 2008; 7:118–131. [PubMed: 19123982]
160. Tsimikas S, Willerson JT, Ridker PM. C-reactive protein and other emerging blood biomarkers to optimize risk stratification of vulnerable patients. J Am Coll Cardiol. 2006; 47:C19–C31. [PubMed: 16631506]

161. Vasan RS. Biomarkers of cardiovascular disease: molecular basis and practical considerations. Circulation. 2006; 113:2335–2362. [PubMed: 16702488]
162. Hirsch LR, Halas NJ, West JL. Whole-blood immunoassay facilitated by gold nanoshell-conjugate antibodies. Methods Mol Biol. 2005; 303:101–111. [PubMed: 15923678]
163. Soman CP, Giorgio TD. Quantum dot self-assembly for protein detection with sub-picomolar sensitivity. Langmuir. 2008; 24:4399–4404. [PubMed: 18335969]
164. Kim KS, Park JK. Magnetic force-based multiplexed immunoassay using superparamagnetic nanoparticles in microfluidic channel. Lab Chip. 2005; 5:657–664. [PubMed: 15915258]
165. Perez JM, Josephson L, O'Loughlin T, Hogemann D, Weissleder R. Magnetic relaxation switches capable of sensing molecular interactions. Nat Biotechnol. 2002; 20:816–820. [PubMed: 12134166]
166. Hirsch LR, Jackson JB, Lee A, Halas NJ, West JL. A whole blood immunoassay using gold nanoshells. Anal Chem. 2003; 75:2377–2381. [PubMed: 12918980]
167. Blinka E, Loeffler K, Hu Y, Gopal A, Hoshino K, Lin K, Liu X, Ferrari M, Zhang JX. Enhanced micro-contact printing of proteins on nanoporous silica surface. Nanotechnology. 2010; 21:415302. [PubMed: 20834118]
168. Agrawal A, Sathe T, Nie S. Single-bead immunoassays using magnetic microparticles and spectral-shifting quantum dots. J Agric Food Chem. 2007; 55:3778–3782. [PubMed: 17455953]
169. Bulte, JWM., Modo, MMJ., Perez, JM., Kaittanis, C. Magnetic nanosensors for probing molecular interactions. In: Ferrari, M., editor. Nanoparticles in Biomedical Imaging. Vol. 102. New York: Springer; 2008. p. 183-197.
170. Ibraimi F, Kriz D, Lu M, Hansson L-O, Kriz K. Rapid one-step whole blood C-reactive protein magnetic permeability immunoassay with monoclonal antibody conjugated nanoparticles as superparamagnetic labels and enhanced sedimentation. Anal Bioanal Chem. 2006; 384:651–657. [PubMed: 16240109]
171. Ng AH, Uddayasankar U, Wheeler AR. Immunoassays in microfluidic systems. Anal Bioanal Chem. 2010; 397:991–1007. [PubMed: 20422163]
172. Jokerst JV, Raamanathan A, Christodoulides N, Floriano PN, Pollard AA, Simmons GW, Wong J, Gage C, Furmaga WB, Redding SW, et al. Nano-bio-chips for high performance multiplexed protein detection: determinations of cancer biomarkers in serum and saliva using quantum dot bioconjugate labels. Biosens Bio-electron. 2009; 24:3622–3629.
173. Sia SK, Whitesides GM. Microfluidic devices fabricated in poly(dimethylsiloxane) for biological studies. Electrophoresis. 2003; 24:3563–3576. [PubMed: 14613181]
174. McClain MA, Culbertson CT, Jacobson SC, Ramsey JM. Flow cytometry of *Escherichia coli* on microfluidic devices. Anal Chem. 2001; 73:5334–5338. [PubMed: 11721938]
175. Wlodkowic D, Faley S, Zagnoni M, Wikswo JP, Cooper JM. Microfluidic single-cell array cytometry for the analysis of tumor apoptosis. Anal Chem. 2009; 81:5517–5523. [PubMed: 19514700]
176. Adams ML, Enzelberger M, Quake S, Scherer A. Microfluidic integration on detector arrays for absorption and fluorescence micro-spectrometers. Sensors Actuat A Phys. 2003; 104:25–31.
177. Haun JB, Yoon TJ, Lee H, Weissleder R. Magnetic nanoparticle biosensors. Wiley Interdiscip Rev Nanomed Nanobiotechnol. 2010; 2:291–304. [PubMed: 20336708]
178. Lee H, Sun E, Ham D, Weissleder R. Chip-NMR biosensor for detection and molecular analysis of cells. Nat Med. 2008; 14:869–874. [PubMed: 18607350]
179. Chastek TQ, Beers KL, Amis EJ. Miniaturized dynamic light scattering instrumentation for use in microfluidic applications. Rev Sci Instrum. 2007; 78:072201. [PubMed: 17672732]
180. Chastek TQ, Iida K, Amis EJ, Fasolka MJ, Beers KL. A microfluidic platform for integrated synthesis and dynamic light scattering measurement of block copolymer micelles. Lab Chip. 2008; 8:950–957. [PubMed: 18497917]
181. Soman C, Giorgio T. Sensitive and multiplexed detection of proteomic antigens via quantum dot aggregation. Nanomed: Nanotechnol Biol Med. 2009; 5:402–409.
182. Wyatt PJ. Light-Scattering and the absolute characterization of macromolecules. Anal Chim Acta. 1993; 272:1–40.

183. Oden M, Mirabal Y, Epstein M, Richards-Kortum R. Engaging undergraduates to solve global health challenges: a new approach based on bioengineering design. Ann Biomed Eng. 2010; 38:3031–3041. [PubMed: 20387116]

184. Bruls DM, Evers TH, Kahlman JAH, van Lankvelt PJW, Ovsyanko M, Pelssers EGM, Schleipen JJHB, de Theije FK, Verschuren CA, van der Wijk T, et al. Rapid integrated biosensor for multiplexed immunoassays based on actuated magnetic nanoparticles. Lab Chip. 2009; 9:3504–3510. [PubMed: 20024029]

185. Floriano PN, Christodoulides N, Miller CS, Ebersole JL, Spertus J, Rose BG, Kinane DF, Novak MJ, Steinhubl S, Acosta S, et al. Use of saliva-based nano-biochip tests for acute myocardial infarction at the point of care: a feasibility study. Clin Chem. 2009; 55:1530–1538. [PubMed: 19556448]

186. Lavigne JJ, Savoy S, Clevenger MB, Ritchie JE, McDoniel B, Yoo S-J, Anslyn EV, McDevitt JT, Shear JB, Neikirk D. Solution-based analysis of multiple analytes by a sensor array: toward the development of an “electronic tongue”. J Am Chem Soc. 1998; 120:6429–6430.

187. Buch M, Rishpon J. An electrochemical immunosensor for C-reactive protein based on multi-walled carbon nanotube-modified electrodes. Electroanalysis. 2008; 20:2592–2594.

188. Wang J. Carbon-nanotube based electrochemical biosensors: a review. Electroanalysis. 2005; 17:7–14.

189. Gruntzig AR, Senning A, Siegenthaler WE. Nonoperative dilatation of coronary-artery stenosis: percutaneous transluminal coronary angioplasty. N Engl J Med. 1979; 301:61–68. [PubMed: 449946]

190. de Feyter PJ, de Jaegere PP, Serruys PW. Incidence, predictors, and management of acute coronary occlusion after coronary angioplasty. Am Heart J. 1994; 127:643–651. [PubMed: 8122614]

191. Sigwart U, Urban P, Golf S, Kaufmann U, Imbert C, Fischer A, Kappenberger L. Emergency stenting for acute occlusion after coronary balloon angioplasty. Circulation. 1988; 78:1121–1127. [PubMed: 3180371]

192. Sigwart U, Puel J, Mirkovitch V, Joffre F, Kappen-berger L. Intravascular stents to prevent occlusion and restenosis after transluminal angioplasty. N Engl J Med. 1987; 316:701–706. [PubMed: 2950322]

193. Moliterno DJ. Healing achilles—sirolimus versus paclitaxel. N Engl J Med. 2005; 353:724–727. [PubMed: 16105991]

194. Karas SP, Gravanis MB, Santoian EC, Robinson KA, Anderberg KA, King SB 3rd. Coronary intimal proliferation after balloon injury and stenting in swine: an animal model of restenosis. J Am Coll Cardiol. 1992; 20:467–474. [PubMed: 1634687]

195. Gordon PC, Gibson CM, Cohen DJ, Carrozza JP, Kuntz RE, Baim DS. Mechanisms of restenosis and redilation within coronary stents—quantitative angiographic assessment. J Am Coll Cardiol. 1993; 21:1166–1174. [PubMed: 8459072]

196. Hoffmann R, Mintz GS, Dussaillant GR, Popma JJ, Pichard AD, Satler LF, Kent KM, Griffin J, Leon MB. Patterns and mechanisms of in-stent restenosis. a serial intravascular ultrasound study. Circulation. 1996; 94:1247–1254. [PubMed: 8822976]

197. Babapulle MN, Joseph L, Belisle P, Brophy JM, Eisenberg MJ. A hierarchical Bayesian meta-analysis of randomised clinical trials ofdrug-elutingstents. Lancet. 2004; 364:583–591. [PubMed: 15313358]

198. Stone GW, Ellis SG, Cox DA, Hermiller J, O’Shaughnessy C, Mann JT, Turco M, Caputo R, Bergin P, Greenberg J, et al. One-year clinical results with the slow-release, polymer-based, paclitaxel-eluting TAXUS stent: the TAXUS-IV trial. Circulation. 2004; 109:1942–1947. [PubMed: 15078803]

199. Moses JW, Leon MB, Popma JJ, Fitzgerald PJ, Holmes DR, O’Shaughnessy C, Caputo RP, Kereiakes DJ, Williams DO, Teirstein PS, et al. Sirolimus-eluting stents versus standard stents in patients with stenosis in a native coronary artery. N Engl J Med. 2003; 349:1315–1323. [PubMed: 14523139]

200. Nordmann AJ, Briel M, Bucher HC. Mortality in randomized controlled trials comparing drug-eluting vs. bare metal stents in coronary artery disease: a meta-analysis. Eur Heart J. 2006; 27:2784–2814. [PubMed: 17020889]

201. Camenzind E, Steg PG, Wijns W. Stent thrombosis late after implantation of first-generation drug-eluting stents: a cause for concern. Circulation. 2007; 115:1440–1455. discussion 1455. [PubMed: 17344324]

202. Lagerqvist B, James SK, Stenestrand U, Lindback J, Nilsson T, Wallentin L. Long-term outcomes with drug-eluting stents versus bare-metal stents in Sweden. N Engl J Med. 2007; 356:1009–1019. [PubMed: 17296822]

203. Kastrati A, Dibra A, Eberle S, Mehilli J, Suarez de Lezo J, Goy JJ, Ulm K, Schomig A. Sirolimus-eluting stents vs paclitaxel-eluting stents in patients with coronary artery disease: meta-analysis of randomized trials. JAMA. 2005; 294:819–825. [PubMed: 16106007]

204. Niccoli G, Montone RA, Ferrante G, Crea F. The evolving role of inflammatory biomarkers in risk assessment after stent implantation. J Am Coll Cardiol. 2010; 56:1783–1793. [PubMed: 21087705]

205. Kastrati A, Mehilli J, Dirschinger J, Dotzer F, Schuhlen H, Neumann FJ, Fleckenstein M, Pfafferott C, Seyfarth M, Schomig A. Intracoronary stenting and angiographic results: strut thickness effect on restenosis outcome (ISAR-STEREO) trial. Circulation. 2001; 103:2816–2821. [PubMed: 11401938]

206. Pache J, Kastrati A, Mehilli J, Schuhlen H, Dotzer F, Hausleiter J, Fleckenstein M, Neumann FJ, Sattel-berger U, Schmitt C, et al. Intracoronary stenting and angiographic results: strut thickness effect on restenosis outcome (ISAR-STEREO-2) trial. J Am Coll Cardiol. 2003; 41:1283–1288. [PubMed: 12706922]

207. Kereiakes DJ, Cox DA, Hermiller JB, Midei MG, Bachinsky WB, Nukta ED, Leon MB, Fink S, Marin L, Lansky AJ. Usefulness of a cobalt chromium coronary stent alloy. Am J Cardiol. 2003; 92:463–466. [PubMed: 12914881]

208. Stone GW, Rizvi A, Newman W, Mastali K, Wang JC, Caputo R, Doostzadeh J, Cao S, Simonton CA, Sudhir K, et al. Everolimus-eluting versus paclitaxel-eluting stents in coronary artery disease. New Engl J Med. 2010; 362:1663–1674. [PubMed: 20445180]

209. Byrne RA, Kufner S, Tiroch K, Massberg S, Laugwitz KL, Birkmeier A, Schulz S, Mehilli J. Randomised trial of three rapamycin-eluting stents with different coating strategies for the reduction of coronary restenosis: 2-year follow-up results. Heart. 2009; 95:1489–1494. [PubMed: 19592388]

210. Byrne RA, Mehilli J, Iijima R, Schulz S, Pache J, Seyfarth M, Schomig A, Kastrati A. A polymer-free dual drug-eluting stent in patients with coronary artery disease: a randomized trial vs. polymer-based drug-eluting stents. Eur Heart J. 2009; 30:923–931. [PubMed: 19240066]

211. Tamai H, Igaki K, Kyo E, Kosuga K, Kawashima A, Matsui S, Komori H, Tsuji T, Motohara S, Uehata H. Initial and 6-month results of biodegradable poly-l-lactic acid coronary stents in humans. Circulation. 2000; 102:399–404. [PubMed: 10908211]

212. Tsuji T, Tamai H, Igaki K, Hsu Y-S, Kosuga KMO, Nakamura T, Fujita S. Four-year follow-up of the biodegradable stent (IGAKI-TAMAI Stent). Circ J. 2004; 68:135. [PubMed: 14745148]

213. Erbel R, Di Mario C, Bartunek J, Bonnier J, de Bruyne B, Eberli FR, Erne P, Haude M, Heublein B, Horrigan M, et al. Temporary scaffolding of coronary arteries with bioabsorbable magnesium stents: a prospective, non-randomised multicentre trial. Lancet. 2007; 369:1869–1875. [PubMed: 17544767]

214. Ormiston JA, Serruys PW, Regar E, Dudek D, Thuesen L, Webster MW, Onuma Y, Garcia-Garcia HM, McGreevy R, Veldhof S. A bioabsorbable everolimus-eluting coronary stent system for patients with single de-novo coronary artery lesions (ABSORB): a prospective open-label trial. Lancet. 2008; 371:899–907. [PubMed: 18342684]

215. Serruys PW, Ormiston JA, Onuma Y, Regar E, Gonzalo N, Garcia-Garcia HM, Nieman K, Bruining N, Dorange C, Miquel-Hebert K, et al. A bioabsorbable everolimus-eluting coronary stent system (ABSORB): 2-year outcomes and results from multiple imaging methods. Lancet. 2009; 373:897–910. [PubMed: 19286089]

216. Jiang W-W, Su S-H, Eberhart RC, Tang L. Phagocyte responses to degradable polymers. J Biomed Mater Res A. 2007; 82A:492–497.
217. Ramcharitar S, Gonzalo N, van Geuns RJ, Garcia-Garcia HM, Wykrzykowska JJ, Ligthart JMR, Regar E, Serruys PW. First case of stenting of a vulnerable plaque in the SECRITT I trial—the dawn of a new era? Nat Rev Cardiol. 2009; 6:374–378. [PubMed: 19377499]
218. O'Brien B, Carroll W. The evolution of cardiovascular stent materials and surfaces in response to clinical drivers: A review. Acta Biomater. 2009; 5:945–958. [PubMed: 19111513]
219. Virmani R, Guagliumi G, Farb A, Musumeci G, Grieco N, Motta T, Mihalcsik L, Tespili M, Valsecchi O, Kolodgie FD. Localized hypersensitivity and late coronary thrombosis secondary to a sirolimus-eluting stent should we be cautious? Circulation. 2004; 109:701–705. [PubMed: 14744976]
220. Kuchulakanti PK, Chu WW, Torguson R, Ohlmann P, Rha SW, Clavijo LC, Kim SW, Bui A, Gevorkian N, Xue ZY, et al. Correlates and long-term outcomes of angiographically proven stent thrombosis with sirolimus- and paclitaxel-eluting stents. Circulation. 2006; 113:1108–1113. [PubMed: 16490815]
221. Joner M, Finn AV, Farb A, Mont EK, Kolodgie FD, Ladich E, Kutys R, Skorija K, Gold HK, Virmani R. Pathology of drug-eluting stents in humans—delayed healing and late thrombotic risk. J Am Coll Cardiol. 2006; 48:193–202. [PubMed: 16814667]
222. Tada DB, Singh S, Nagesha D, Jost E, Levy CO, Gultepe E, Cormack R, Makrigiorgos GM, Sridhar S. Chitosan film containing Poly(D,L-Lactic-Co-glycolic acid) nanoparticles: a platform for localized dual-drug release. Pharma Res. 2010; 27:1738–1745.
223. Jayagopal A, Sussman EM, Shastri VP. Functionalized solid lipid nanoparticles for transendothelial delivery. IEEE Trans Nanobiosci. 2008; 7:28–34.
224. Jin C, Bai L, Wu H, Song W, Guo GZ, Dou KF. Cyto-toxicity of paclitaxel incorporated in PLGA nanoparticles on hypoxic human tumor cells. Pharma Res. 2009; 26:1776–1784.
225. Ranganath SH, Kee I, Krantz WB, Chow PKH, Wang CH. Hydrogel matrix entrapping PLGA-paclitaxel microspheres: drug delivery with near zero-order release and implantability advantages for malignant brain tumour chemotherapy. Pharma Res. 2009; 26:2101–2114.
226. Bhargava B, Reddy NK, Karthikeyan G, Raju R, Mishra S, Singh S, Waksman R, Virmani R, Somaraju B. A novel paclitaxel-eluting porous carboncarbon nanoparticle coated, nonpolymeric cobalt-chromium stent: evaluation in a porcine model. Cathet Cardiovasc Intervent. 2006; 67:698–702.
227. Kushwaha M, Anderson JM, Bosworth CA, Andukuri A, Minor WP, Lancaster JR, Anderson PG, Brott BC, Jun HW. A nitric oxide releasing, self assembled peptide amphiphile matrix that mimics native endothelium for coating implantable cardiovascular devices. Biomaterials. 2010; 31:1502–1508. [PubMed: 19913295]
228. Andukuri A, Minor WP, Kushwaha M, Anderson JM, Jun HW. Effect of endothelium mimicking self-assembled nanomatrices on cell adhesion and spreading of human endothelial cells and smooth muscle cells. Nanomed Nanotechnol Biol Med. 2010; 6:289–297.
229. Decher G. Fuzzy nanoassemblies: toward layered polymeric multicomposites. Science. 1997; 277:1232–1237.
230. Soike T, Streff AK, Guan CX, Ortega R, Tantawy M, Pino C, Shastri VP. Engineering a material surface for drug delivery and imaging using layer-by-layer assembly of functionalized nanoparticles. Adv Mater. 2010; 22:1992.
231. Weber N, Pesnell A, Bolikal D, Zeltinger J, Kohn J. Viscoelastic properties of fibrinogen adsorbed to the surface of biomaterials used in blood-contacting medical devices. Langmuir. 2007; 23:3298–3304. [PubMed: 17291015]
232. Otsuka M, Tanimoto S, Sianos G, Kukreja N, Weustink AC, Serruys PW, De Feyter PJ. "Radio-lucent" and "radio-opaque" coronary stents characterized by multislice computed tomography. Int J Cardiol. 2009; 132:E8–E10. [PubMed: 17977611]
233. Luscher TF, Steffel J, Eberli FR, Joner M, Nakazawa G, Tanner FC, Virmani R. Drug-eluting stent and coronary thrombosis: biological mechanisms and clinical implications. Circulation. 2007; 115:1051–1058. [PubMed: 17325255]

234. Daemen J, Wenaweser P, Tsuchida K, Abrecht L, Vaina S, Morger C, Kukreja N, Juni P, Sianos G, Hellige G, et al. Early and late coronary stent thrombosis of sirolimus-eluting and paclitaxel-eluting stents in routine clinical practice: data from a large two-institutional cohort study. Lancet. 2007; 369:667–678. [PubMed: 17321312]

235. Peng L, Eltgroth ML, LaTempa TJ, Grimes CA, Desai TA. The effect of TiO_2 nanotubes on endothelial function and smooth muscle proliferation. Biomaterials. 2009; 30:1268–1272. [PubMed: 19081625]

236. Lu J, Rao MP, MacDonald NC, Khang D, Webster TJ. Improved endothelial cell adhesion and proliferation on patterned titanium surfaces with rationally designed, micrometer to nanometer features. Acta Biomater. 2008; 4:192–201. [PubMed: 17851147]

237. Miller DC, Thapa A, Haberstroh KM, Webster TJ. Endothelial and vascular smooth muscle cell function on poly(lactic-co-glycolic acid) with nanostructured surface features. Biomaterials. 2004; 25:53–61. [PubMed: 14580908]

238. Fine E, Zhang L, Fenniri H, Webster TJ. Enhanced endothelial cell functions on rosette nanotube-coated titanium vascular stents. Int J Nanomed. 2009; 4:91–97.

239. Kipshidze N, Dangas G, Tsapenko M, Moses J, Leon MB, Kutryk M, Serruys P. Role of the endothelium in modulating neointimal formation: vasculoprotective approaches to attenuate restenosis after percutaneous coronaryinterventions. J Am Coll Cardiol. 2004; 44:733–739. [PubMed: 15312851]

240. Lu J, Khang D, Webster TJ. Greater endothelial cell responses on submicron and nanometer rough titanium surfaces. J Biomed Mater Res A. 2010; 94A:1042–1049.

241. Khang D, Kim SY, Liu-Snyder P, Palmore GTR, Durbin SM, Webster TJ. Enhanced fibronectin adsorption on carbon nanotube/poly(carbonate) urethane: independent role of surface nano-roughness and associated surface energy. Biomaterials. 2007; 28:4756–4768. [PubMed: 17706277]

242. Loya MC, Brammer KS, Choi C, Chen LH, Jin SH. Plasma-induced nanopillars on bare metal coronary stent surface for enhanced endothelialization. Acta Biomater. 2010; 6:4589–4595. [PubMed: 20624494]

243. Brammer KS, Choi C, Oh S, Cobb CJ, Connelly LS, Loya M, Kong SD, Jin S. Antibiofouling, sustained antibiotic release by Si nanowire templates. Nano Lett. 2009; 9:3570–3574. [PubMed: 19637854]

244. Samaroo HD, Lu J, Webster TJ. Enhanced endothelial cell density on NiTi surfaces with sub-macron to nanometer roughness. Int J Nanomed. 2008; 3:75–82.

245. Wieneke H, Dirsch O, Sawitowski T, Gu YL, Brauer H, Dahmen U, Fischer A, Wnendt S, Erbel R. Synergistic effects of a novel nanoporous stent coating and tacrolimus on intima proliferation in rabbits. Cathet Cardiovasc Intervent. 2003; 60:399–407.

FURTHER READING

246. Buxton DB. Current status of nanotechnology approaches for cardiovascular disease: a personal perspective. WIREs Nanomed Nanobiotechnol. 2009; 1:149–155.

247. Jarzyna PA, Gianella A, Skajaa T, Knudsen G, Deddens LH, Cormode DP, Fayad ZA, Mulder WJM. Multifunctional imaging nanoprobes. WIREs Nanomed Nanobiotechnol. 2010; 2:138–150.

248. Puskas JE, Muñoz-Robledo LG, Hoerr RA, Foley J, Schmidt SP, Evancho-Chapman M, Dong J, Frethem C, Haugstad G. Drug eluting stent coatings. WIREs Nanomed Nanobiotechnol. 2009; 1:451–462.

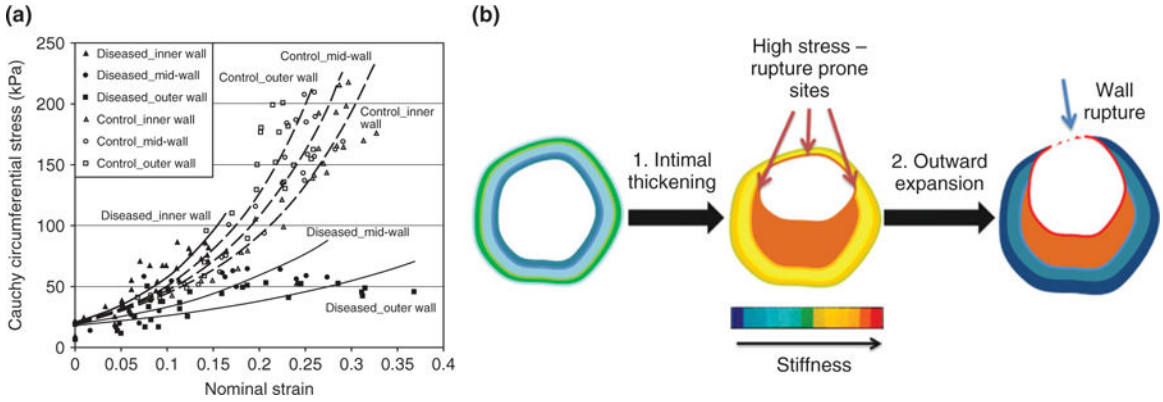

FIGURE 1.

Changes in mechanical properties of the vascular wall as a result of pathological vascular remodeling. (a) *Ex vivo* stress—strain curves of porcine plaque-laden versus healthy vascular tissue. All samples were taken from the left anterior descending coronary artery in juvenile pigs, with atherosclerosis induced via standard balloon angioplasty injury. Control samples were obtained from pigs without induced injury. (Reprinted with permission from Ref 24. Copyright 2003 ASME Publications.) (b) Schematic of changes in layer-by-layer stiffness during progression of pathological vascular remodeling. Pathological changes that decrease the lumen of a remodeling artery include intimal thickening and constrictive geometric remodeling of the wall, leading to a significant increase in the stiffness of inner layer, while vessel wall rupture that is resulted from artery expansion to increase the lumen for restoration of proper blood flow leads to decreased stiffness of middle and outer layers.

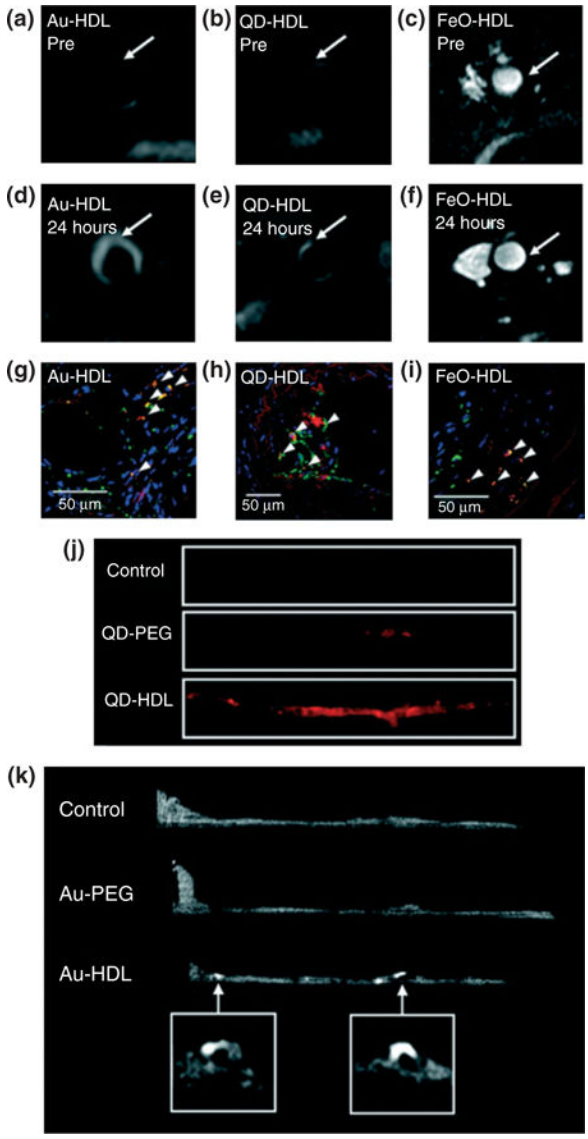

FIGURE 2.

Multimodality imaging of atherosclerosis using nanocrystals encapsulated in high density lipoprotein. T1-weighted MR images of the aorta of apoE KO mice pre- (a and b) and 24 h postinjection (d and e) with Au-HDL or QD-HDL. Arrows indicate areas enhanced in the post images. (c and f) T2*-weighted images of an apoE KO mouse pre- and 24 h postinjection with FeO-HDL. (g–i) Confocal microscopy images of aortic sections of mice injected with nanocrystal HDL. Red is nanocrystal HDL, macrophages are green, and nuclei are blue. Yellow indicates colocalization of nanocrystal HDL with macrophages and is indicated by arrowheads. (j) Fluorescence image of aortas of mice injected with QD-HDL, QDPEG, and saline. (k) *Ex vivo* sagittal CT images of the aortas of mice injected with Au-HDL, Au-PEG, and saline. (Reprinted with permission from Ref 95. Copyright 2008 American Chemical Society)

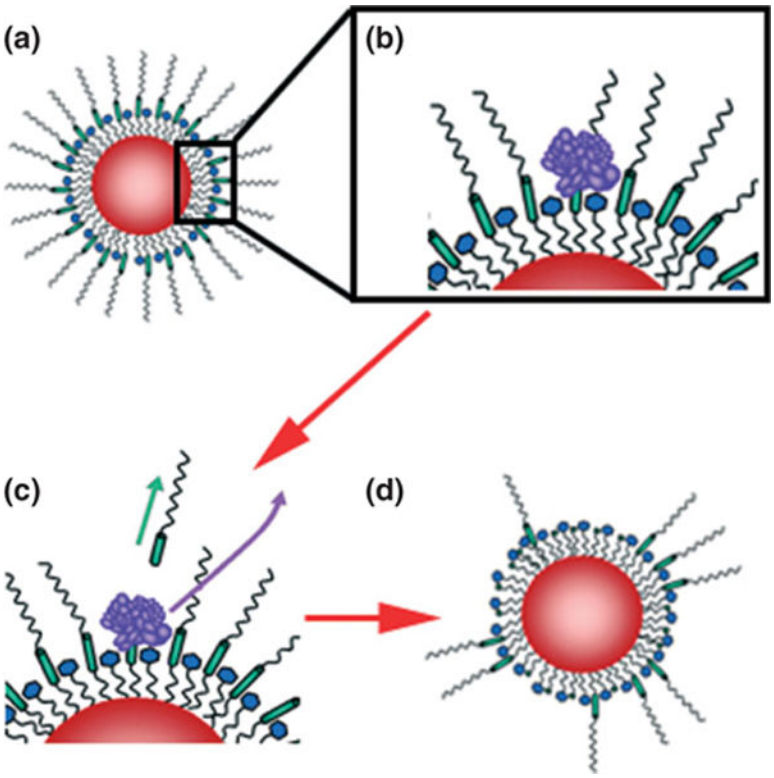

FIGURE 3.

Dual-ligand, protease-activatable quantum dots for imaging applications. In 'Proximity Activated Targeting' (PAT) the targeting ligand (blue) is initially concealed (a) until proteolytic activity through tumor-secreted MMPs (purple) cleaves a peptide bridge (green) within long chain PEGs. Subsequent diffusion of the MMP and cleavage fragments (c) reveals the ligand-targeted construct only in the proximity of the tumor (d).

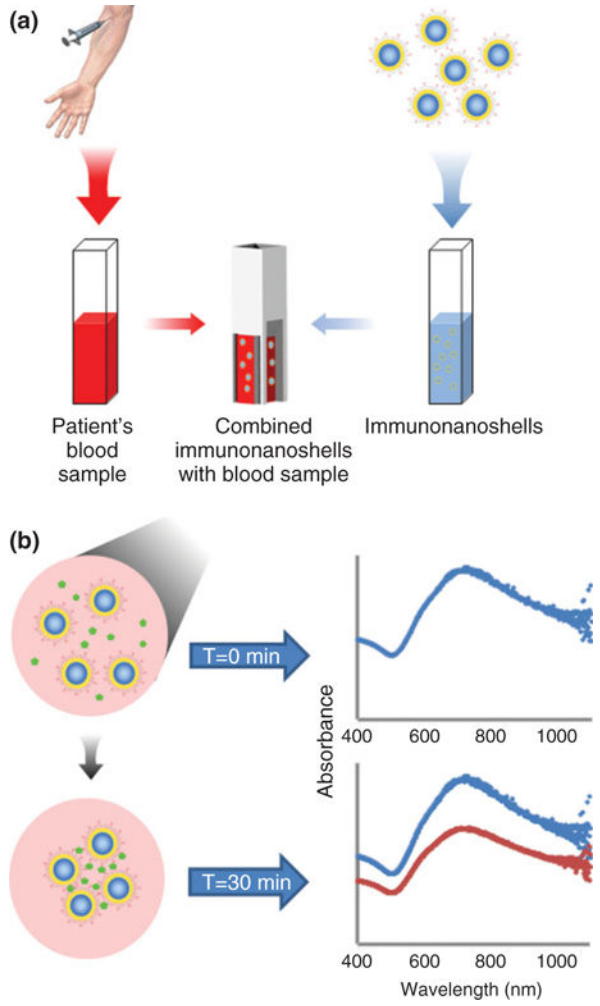

FIGURE 4.

Nanoshell immunoassay. (a) In concept, the nanoshell immunoassay is designed to enable rapid and accurate analyte concentration measurements in whole blood, while minimizing dependency on long sample handling and instrumentation typified by standard immunoassays.[166] (b) Absorbance spectra of nanoshells prior to versus 30 min after analyte addition. Peak absorbance is estimated at 725 nm. A decrease in material extinction coefficient is observed as a result of clustering of the nanoshells.

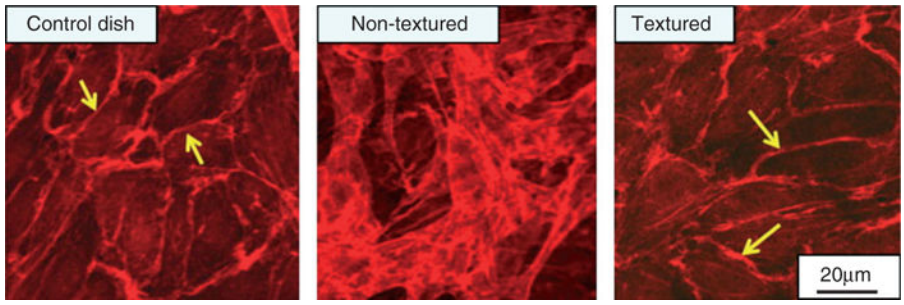

FIGURE 5.

Bovine aortic endothelial cell adhesion and function on nanotextured versus conventional MP35N surfaces. Actin staining on a control dish (plastic), non-nanotextured and nanotextured MP35N surfaces. The presence of peri-junctional cortical bands of filamentous actin are clearly visible (arrows) on both the control and textured surfaces, but are not as pronounced on the nontextured surface, showing multiple layers of possibly aggregated cells. (Reprinted with permission from Ref 242. Copyright 2008 Elsevier)

TABLE 1

Nanoparticle-Mediated *In Vivo*/*Ex Vivo* Imaging of Atherosclerosis Related Biomarkers

Molecular/ Cellular Target	Nanoparticle Type	Targeting Motif	Imaging Modality	Animal Models[1]	References
Cathepsins (nonspecific activity probe)	Polyethylene glycol-poly-lysine	Degradable peptide	FMT, CT	apoE$^{-/-}$ mice	86
Dextran receptors (macrophages)	Au-coated iron oxide nanoroses	Dextran surface coating	Hyperspectral microscopy (3d post-injection, harvested aorta)	New Zealand white rabbits, cholesterol-fed + balloon injury	87
E-selectin	Iron oxide	Anti-human CD62E F(ab')2	T_2-weighted MRI	Athymic female *nu/nu* mice	88 and 89
Fibrin	Lipid-stabilized perfluorocarbon emulsion	Anti-fibrin Mab	T_1-weighted MRI	Dog, induced thrombus in open circulation	90
Fibrin	Synthetic phospholipid micelle	CREKA peptide	Fluorescence imaging	apoE$^{-/-}$ mice	91
HDL receptors / transporters	Modified HDL mimic with Au, iron oxide, or quantum dots	Apo-A1	Multimodal; CT, MRI, Fluorescence	apoE$^{-/-}$ mice	92–95
Macrophages	Sinerem (AMAG Pharmaceuticals, Lexington, MA)	Nonspecific binding	T_2-weighted MRI	human	46 and 96
Macrophages	Iron oxide (dextran coated)	Nonspecific binding	T_2-weighted MRI	New Zealand white rabbits, cholesterol-fed + balloon injury	97
Macrophages	Au, mPEG-stabilized	Nonspecific binding	Intravascular photoacoustic/intravascular ultrasound	Excised rabbit aortas; cholesterol-fed (ex *vivo)*	98
Macrophages	Poloxamer-stabilized iodine	Nonspecific binding	CT	New Zealand white rabbits, cholesterol-fed + balloon injury	99 and 100
MMP-2	Iron oxide	MMP-2-degradable peptide	T_2-weighted MRI	Nude mice/HT-1080 tumor cell injection	101
MMP-9	Iron oxide	MMP-9-degradable peptide	T_2-weighted MRI	None	102
Malondialdehydelysine, oxidized phospholipids	Gd-oriron oxide-containing micelles	Antibodies against oxidation-specific epitopes	MRI, fluorescence	apoE$^{-/-}$ mice	103 and 104
Phosphatidylserine (apoptotic/necrotic cells)	Gd- and rhodamine-tagged micelles	Annexin A5	T_1-weighted MRI, Fluorescence	apoE$^{-/-}$ mice	105
Reactive oxygen species	Peroxalate polymer nanoparticles	Peroxide-sensitive peroxalate linkages	Chemiluminescence	C57Bl/6 mice	106
SR-A (macrophage scavenger receptor A)	Gd-containing micelles	Anti-murine CD204 IgG	T_1-weighted MRI, Fluorescence	apoE$^{-/-}$ mice	107 and 108
SR-B (macrophage scavenger receptor B)	Gd-containing micelles	Anti-human CD36 IgG	T_1-weighted MRI, Fluorescence	human (ex *vivo)*	47
VCAM-1	Iron oxide (dextran-coated)	Peptide, Anti-VCAM-1 Ab	T_2-weighted MRI, Fluorescence	apoE$^{-/-}$ mice, C57Bl/6 mice	109–111
$\alpha_V\beta_3$ integrins	Lipid-stabilized perfluorocarbon emulsion	RGD peptide	T_1-weighted MRI	New Zealand white rabbits, cholesterol-fed	112

[1]All models noted are *in vivo* unless otherwise noted.

TABLE 2

Technical Specifications of Representative Clinically Approved Drug-Eluting Stents in the United States and Europe

Coating	Stent	Drug	Polymer	Stent Platform	Strut/coating Thickness (μm)	Approval
Durable polymer	CYPHER	Sirolimus	Polyethylene *co*-vinyl acetate and poly-*n*-butyl methacrylate	SS	140/12.6	FDA/CE
	TAXUS Express	Paclitaxel	Poly(styrene-*b*-isobutylene-*b*-styrene)	SS	132/16	FDA/CE
	TAXUS Liberte'	Paclitaxel	Poly(styrene-*b*-isobutylene-*b*-styrene)	SS	97/16	FDA/CE
	Endeavor	Zotarolimus	Phosphorylcholine	CoCr	91/4.1	FDA/CE
	Xience V	Everolimus	Polyvinylidene fluoride *co*-hexafluoropropylene and poly-*n*-butyl methacrylate	CoCr	81/7.6	FDA/CE
	Endeavor RESOLUTE	Zotarolimus	C10/C19/polyvinyl pyrrolidone	CoCr	91/4.1	CE
	Promus element	Everolimus	Polyvinylidene fluoride co-hexafluoropropylene and poly-*n*-butyl methacrylate	PtCr	81/6	CE
Biodegradable polymer	NOBORI	Biolimus A9	Abluminal poly-L-Lactide	SS	112/10[1]	CE
	Axxess	Biolimus A9	Abluminal poly-L-Lactide	Nitinol	152/15[1]	CE
	BioMatrix	Biolimus A9	Abluminal poly-L-Lactide	SS	112/10[1]	CE
	XTENT	Biolimus A9	Abluminal poly-L-Lactide	CoCr	NA	CE
Polymer free	Yukon Choice	Sirolimus	None	SS	87	CE
	Amazonia Pax	Paclitaxel	None	CoCr	73/5[1]	CE
Bioabsorbable/biodegradable stents	Igaki-Tamai	None	None	Poly-lactic acid	170/NA	CE
	ABSORB	Everolimus	Poly-D,L-lactide	Poly-lactic acid	150/6	CE

FDA, Food and Drug Administration; CE, Conformité Européene; SS, stainless steel; CoCr, cobalt chromium; PtCr, platinum chromium.

[1]Only abluminal.

Wiley Interdiscip Rev Nanomed Nanobiotechnol. Author manuscript; available in PMC 2017 June 27.